FILE COPY
NO. 3

NATIONAL ADVISORY COMMITTEE FOR AERONAUTICS

REPORT No. 891

A THERMODYNAMIC STUDY OF THE TURBOJET ENGINE

By BENJAMIN PINKEL and IRVING M. KARP

CASE FILE COPY

THIS DOCUMENT ON LOAN FROM THE FILES OF
NATIONAL ADVISORY COMMITTEE FOR AERONAUTICS
LANGLEY AERONAUTICAL LABORATORY
LANGLEY FIELD, HAMPTON, VIRGINIA
RETURN TO THE ABOVE ADDRESS.

REQUESTS FOR PUBLICATIONS SHOULD BE ADDRESSED AS FOLLOWS:
NATIONAL ADVISORY COMMITTEE FOR AERONAUTICS
1724 F STREET, N.W.,
WASHINGTON 25, D.C.

1947

For sale by the Superintendent of Documents, U. S. Government Printing Office, Washington 25, D. C. - - - - - Price 20 cents

AERONAUTIC SYMBOLS

1. FUNDAMENTAL AND DERIVED UNITS

	Symbol	Metric		English	
		Unit	Abbreviation	Unit	Abbreviation
Length	l	meter	m	foot (or mile)	ft (or mi)
Time	t	second	s	second (or hour)	sec (or hr)
Force	F	weight of 1 kilogram	kg	weight of 1 pound	lb
Power	P	horsepower (metric)		horsepower	hp
Speed	V	kilometers per hour	kph	miles per hour	mph
		meters per second	mps	feet per second	fps

2. GENERAL SYMBOLS

W Weight$=mg$

g Standard acceleration of gravity$=9.80665$ m/s^2 or 32.1740 ft/sec^2

m Mass$=\frac{W}{g}$

I Moment of inertia$=mk^2$. (Indicate axis of radius of gyration k by proper subscript.)

μ Coefficient of viscosity

ν Kinematic viscosity

ρ Density (mass per unit volume)

Standard density of dry air, 0.12497 kg-m^{-4}-s^2 at 15° C and 760 mm; or 0.002378 lb-ft^{-4} sec^2

Specific weight of "standard" air, 1.2255 kg/m^3 or 0.07651 lb/cu ft

3. AERODYNAMIC SYMBOLS

S Area

S_w Area of wing

G Gap

b Span

c Chord

A Aspect ratio, $\frac{b^2}{S}$

V True air speed

q Dynamic pressure, $\frac{1}{2}\rho V^2$

L Lift, absolute coefficient $C_L=\frac{L}{qS}$

D Drag, absolute coefficient $C_D=\frac{D}{qS}$

D_0 Profile drag, absolute coefficient $C_{D_0}=\frac{D_0}{qS}$

D_i Induced drag, absolute coefficient $C_{D_i}=\frac{D_i}{qS}$

D_p Parasite drag, absolute coefficient $C_{Dp}=\frac{D_p}{qS}$

C Cross-wind force, absolute coefficient $C_C=\frac{C}{qS}$

i_w Angle of setting of wings (relative to thrust line)

i_t Angle of stabilizer setting (relative to thrust line)

Q Resultant moment

Ω Resultant angular velocity

R Reynolds number, $\rho\frac{Vl}{\mu}$ where l is a linear dimension (e.g., for an airfoil of 1.0 ft chord, 100 mph, standard pressure at 15° C, the corresponding Reynolds number is 935,400; or for an airfoil of 1.0 m chord, 100 mps, the corresponding Reynolds number is 6,865,000)

α Angle of attack

ϵ Angle of downwash

α_o Angle of attack, infinite aspect ratio

α_i Angle of attack, induced

α_a Angle of attack, absolute (measured from zero-lift position)

γ Flight-path angle

REPORT No. 891

A THERMODYNAMIC STUDY OF THE TURBOJET ENGINE

By BENJAMIN PINKEL and IRVING M. KARP

Aircraft Engine Research Laboratory
Cleveland, Ohio

National Advisory Committee for Aeronautics

Headquarters, 1724 F Street NW, Washington 25, D. C.

Created by act of Congress approved March 3, 1915, for the supervision and direction of the scientific study of the problems of flight (U. S. Code, title 49, sec. 241). Its membership was increased to 15 by act approved March 2, 1929. The members are appointed by the President, and serve as such without compensation.

JEROME C. HUNSAKER, Sc. D., Cambridge, Mass., *Chairman*

ALEXANDER WETMORE, Sc. D., Secretary, Smithsonian Institution, *Vice Chairman*

HON. JOHN R. ALISON, Assistant Secretary of Commerce.

VANNEVAR BUSH, Sc. D., Chairman, Research and Development Board, Department of National Defense.

EDWARD U. CONDON, PH. D., Director, National Bureau of Standards.

DONALD B. DUNCAN, Vice Admiral, Deputy Chief of Naval Operations (Air).

R. M. HAZEN, B. S., Chief Engineer, Allison Division, General Motors Corp.

WILLIAM LITTLEWOOD, M. E., Vice President, Engineering, American Airlines System.

THEODORE C. LONNQUEST, Rear Admiral, Assistant Chief for Research and Development, Bureau of Aeronautics, Navy Department.

EDWARD M. POWERS, Major General, United States Air Force, Deputy Chief of Staff, Matériel.

ARTHUR E. RAYMOND, M. S., Vice President, Engineering, Douglas Aircraft Co.

FRANCIS W. REICHELDERFER, Sc. D., Chief, United States Weather Bureau.

CARL SPAATZ, General, Chief of Staff, United States Air Force.

ORVILLE WRIGHT, Sc. D., Dayton, Ohio.

THEODORE P. WRIGHT, Sc. D., Administrator of Civil Aeronautics, Department of Commerce.

HUGH L. DRYDEN, PH. D., *Director of Aeronautical Research*

JOHN W. CROWLEY, JR., B. S., *Associate Director of Aeronautical Research*

JOHN F. VICTORY, LLM., *Executive Secretary*

E. H. CHAMBERLIN, *Executive Officer*

HENRY J. E. REID, Sc. D., Director, Langley Memorial Aeronautical Laboratory, Langley Field, Va.

SMITH J. DEFRANCE, B. S., Director Ames Aeronautical Laboratory, Moffett Field, Calif.

EDWARD R. SHARP, LL. B., Director, Flight Propulsion Research Laboratory, Cleveland Airport, Cleveland, Ohio

---

TECHNICAL COMMITTEES

AERODYNAMICS
POWER PLANTS FOR AIRCRAFT
AIRCRAFT CONSTRUCTION
OPERATING PROBLEMS
SELF-PROPELLED GUIDED MISSILES
INDUSTRY CONSULTING

Coordination of Research Needs of Military and Civil Aviation
Preparation of Research Programs
Allocation of Problems
Prevention of Duplication
Consideration of Inventions

LANGLEY MEMORIAL AERONAUTICAL LABORATORY,
Langley Field, Va.

AMES AERONAUTICAL LABORATORY,
Moffett Field, Calif.

FLIGHT PROPULSION RESEARCH LABORATORY,
Cleveland Airport, Cleveland, Ohio

Conduct, under unified control, for all agencies, of scientific research on the fundamental problems of flight

---

OFFICE OF AERONAUTICAL INTELLIGENCE,
Washington, D. C.

Collection, classification, compilation, and dissemination of scientific and technical information on aeronautics

REPORT No. 891

A THERMODYNAMIC STUDY OF THE TURBOJET ENGINE

By Benjamin Pinkel and Irving M. Karp

SUMMARY

Charts are presented for computing thrust, fuel consumption, and other performance values of a turbojet engine for any given set of operating conditions and component efficiencies. The effects of pressure losses in the inlet duct and the combustion chamber, of variation in physical properties of the gas as it passes through the system, of reheating of the gas due to turbine losses, and of change in mass flow by the addition of fuel are included. The principal performance chart shows the effects of primary variables and correction charts provide the effects of secondary variables and of turbine-loss reheat on the performance of the system.

In order to illustrate some of the turbojet-engine-performance characteristics, the thrust per unit mass rate of air flow and the specific fuel consumption are presented for a wide range of flight and engine operating conditions. It is shown that although thrust per unit mass rate of air flow increases with increased combustion-chamber-outlet temperature, an optimum combustion-chamber-outlet temperature exists for minimum specific fuel consumption. This optimum temperature, in some cases, may be less than the limiting temperature imposed by strength-temperature characteristics of current materials.

The influence of characteristics of a given compressor and turbine on performance of a turbojet engine containing a matched set of these given components is discussed for cases of an engine with a centrifugal-flow compressor and of an engine with an axial-flow compressor.

INTRODUCTION

Some thermodynamic studies have been made of turbojet engines in which equations or charts for obtaining the engine performance are presented and in which performance trends are indicated (references 1 to 4). A study of design and stress limitations relating to turbojet engines is given in reference 5. The purpose of the present report is to provide charts in which a factor indicative of engine performance is given in terms of primary flight and engine operating parameters. From these charts, the engine performance for a given set of primary parameters can be quickly evaluated and an insight is provided into the degree of change of performance possible through change in the parameters. The principal performance chart contains only the primary parameters. The effects of secondary parameters are introduced through a correction factor given in a correction chart.

An insight into some of the performance characteristics of the turbojet engine is obtained from calculated results showing the effects of varying combustion-chamber-outlet temperature and compressor pressure ratio on thrust per unit mass rate of air flow and specific fuel consumption. These results are for constant component efficiencies and for a range of flight-speed and altitude conditions.

Also discussed herein is the matching of components of a turbojet engine. Calculated results that illustrate how the performance characteristics of a given turbojet engine are related to the performance characteristics of its components are presented. Two engines are used in this study, one with a centrifugal-flow compressor and one with an axial-flow compressor. The manner in which the performance of each engine varies as engine operating conditions vary from the design point is also illustrated for the cases of the engine with a fixed-area exhaust nozzle and of the engine with a variable-area exhaust nozzle.

SYMBOLS

The significance of the symbols appearing in the charts and in the subsequent discussion is as follows:

A_n	effective exhaust-nozzle area, (sq ft) (For an isentropic expansion in exhaust nozzle, flow through area A_n is equal to actual mass flow through nozzle.)
a,b,c	factors that measure effects produced by secondary variables
B	ratio of compressor tip speed U to turbine-blade speed u
C_v	velocity coefficient of exhaust nozzle
$c_{p,a}$	specific heat of air at constant pressure at $T_0=519°$ R, 7.73 (Btu/(slug)(°F))
$c_{p,g}$	average specific heat at constant pressure of exhaust gases during expansion process, (Btu/(slug)(°F)) (This term, when used with temperature change accompanying expansion, gives change in enthalpy per unit mass.)
F	net thrust, (lb)
f	fuel-air ratio
h	lower heating value of fuel, (Btu/lb)
J	mechanical equivalent of heat, 778 (ft-lb/Btu)
K_c	compressor slip factor, equal to ratio of compressor-shaft power per unit mass rate of air flow to square of compressor tip speed, 550 P_c/M_aU^2

M_a mass rate of air flow, (slug/sec)

M_g mass rate of gas flow through turbine, (slug/sec)

P_c compressor-shaft horsepower input

P_t turbine-shaft horsepower output

p_0 ambient-air pressure, (lb/sq ft absolute)

p_1 total pressure at compressor inlet, (lb/sq ft absolute)

p_2 total pressure at compressor outlet, (lb/sq ft absolute)

p_4 total pressure at turbine inlet, (lb/sq ft absolute)

$p_{5,s}$ static pressure at turbine outlet, (lb/sq ft absolute)

Δp_d drop in total pressure through inlet duct, (lb/sq ft)

Δp_2 drop in total pressure through combustion chamber due to mechanical obstruction of burners and momentum increase of gases during combustion, (lb/sq ft)

r ratio of drop in total pressure in combustion chamber to total pressure at compressor outlet, $\Delta p_2/p_2$

T_0 ambient-air temperature, (°R)

T_1 compressor-inlet total temperature, (°R)

T_2 compressor-outlet total temperature, (°R)

T_4 combustion-chamber-outlet total temperature, (°R)

thp net thrust horsepower

U compressor tip speed, (ft/sec)

u turbine-blade speed measured at turbine pitch line, (ft/sec)

V_j jet velocity, (ft/sec)

ΔV_j increase in jet velocity due to effect of turbine-loss reheat, (ft/sec)

V_o airplane velocity, (ft/sec)

V_t theoretical turbine-nozzle jet velocity corresponding to isentropic expansion of gas from turbine-inlet total pressure and temperature to turbine-outlet static pressure, (ft/sec),

$$V_t=\sqrt{2Jc_{p,g}T_4\left[1-\left(\frac{p_{5,s}}{p_4}\right)^{\frac{\gamma_g-1}{\gamma_g}}\right]}$$

V_5 axial component of gas velocity at turbine outlet, (ft/sec)

W_f mass flow of fuel, (lb/hr)

X ratio of compressor pressure ratio p_2/p_1 to reference pressure ratio $(p_2/p_1)_{ref}$

Y ratio of ram temperature rise to ambient-air temperature, $V_o^2/2Jc_{p,a}T_0$

Z ratio of compressor-shaft power per unit mass rate of air flow to enthalpy of slug of air at temperature T_0, $550\ P_c/M_aJc_{p,a}T_0$

γ_a ratio of specific heats of air, 1.4

γ_g average value of ratio of specific heats of exhaust gas during expansion process

δ ratio of pressure at any point being considered to standard sea-level pressure of 2116 pounds per square foot, that is, $\delta_0=p_0/2116$, $\delta_1=p_1/2116$, and so forth

ϵ correction factor that accounts for over-all effects produced by secondary variables

η_b combustion efficiency equal to ideal fuel-air ratio required to obtain temperature rise in combustion chamber from T_2 to T_4 divided by actual fuel-air ratio

η_c compressor adiabatic efficiency, that is, ideal power required in adiabatically compressing air from compressor-inlet total temperature and pressure to compressor-outlet total pressure divided by compressor-shaft power

$\eta_{c,p}$ compressor polytropic efficiency equal to logarithm of actual pressure ratio divided by logarithm of isentropic pressure ratio that corresponds to actual temperature ratio

η_t turbine total efficiency, that is, turbine-shaft power divided by ideal power of gas jet expanding adiabatically from turbine-inlet total pressure and temperature to turbine-outlet static pressure less kinetic power corresponding to average axial velocity of gas at turbine outlet,

$$\eta_t=\frac{550P_t}{\frac{1}{2}M_gV_t^2-\frac{1}{2}M_gV_5^2}$$

$\eta_{t,s}$ turbine-shaft efficiency, that is, turbine-shaft power divided by ideal power of gas jet expanding adiabatically from turbine-inlet total pressure and temperature to turbine-outlet static pressure,

$$\eta_{t,s}=\frac{550P_t}{\frac{1}{2}M_gV_t^2}$$

θ ratio of temperature at any point being considered to standard sea-level temperature of 519° R, that is, $\theta_0=T_0/519$, $\theta_1=T_1/519$, and so forth

$$(p_2/p_1)_{ref}=\left[\left(\frac{1}{1+Y}\right)^2\eta_c\eta_t\epsilon\,\frac{T_4}{T_0}\right]^{\frac{\gamma_a}{2(\gamma_a-1)}}$$

When variation in ϵ with pressure ratio is negligible, then $(p_2/p_1)_{ref}$ is equal to compressor pressure ratio for maximum thrust per unit mass rate of air flow.

METHOD OF EVALUATING TURBOJET-ENGINE PERFORMANCE

ANALYSIS

A schematic diagram of the turbojet engine considered is shown in figure 1. Air enters the inlet duct and passes to the compressor inlet. Part of the dynamic pressure of the free-air stream is converted into static pressure at the compressor inlet by the diffusing action of the inlet duct. The air is

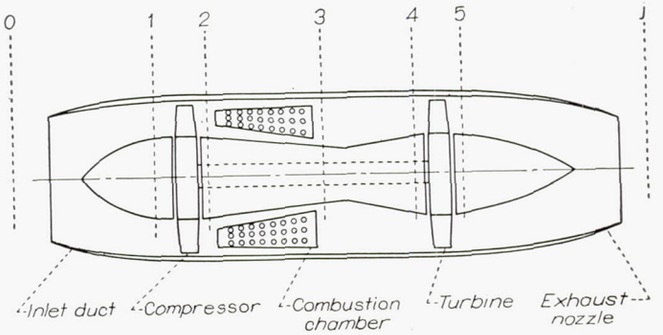


FIGURE 1.—Schematic diagram of turbojet engine.

further compressed in passing through the compressor and enters the combustion chamber where fuel is injected and burned. The products of combustion then pass through the turbine nozzles and blades where an appreciable drop in pressure occurs and finally are discharged rearwardly through the exhaust nozzle to provide thrust.

The variables affecting the performance of the turbojet engine are divided into a primary group and a secondary group. The variables of the primary group are shown on the principal chart for determining the performance of the engine. The variables of the secondary group are shown on a correction chart for determining the factor ϵ, usually close to unity, which also appears as a variable on the principal performance chart.

The primary group of variables consists of:

(a) Compressor adiabatic efficiency η_c
(b) Turbine total efficiency η_t
(c) Burner efficiency η_b
(d) Exhaust-nozzle velocity coefficient C_v, which includes losses in tail pipe
(e) Airplane velocity V_o
(f) Compressor total-pressure ratio p_2/p_1
(g) Ambient-air temperature T_0
(h) Combustion-chamber-outlet total temperature T_4

The secondary group consists of:

(a) Ratio of total-pressure drop through inlet duct caused by friction and turbulence to compressor-inlet total pressure $\Delta p_d/p_1$
(b) Ratio of total-pressure drop through combustion chamber caused by mechanical obstruction of burners and by momentum increase of gases during combustion to compressor-outlet total pressure $\Delta p_2/p_2$
(c) Effect of difference between physical properties of cold air and hot exhaust gases during expansion processes

(The effect of change in specific heat of gas during other processes is included in the charts.)

Charts are presented from which thrust, thrust horsepower, and fuel-air ratio can be evaluated for various combinations of design and operating conditions. The equations from which the charts were prepared are listed in appendix A and are derived in appendix B. The following equations used in combination with the charts give the performance of the turbojet system.

The net thrust of the turbojet engine, when the effect of the added fuel is neglected, is given by the equation

$$F=M_a(V_j-V_o) \tag{1a}$$

When the effect of added fuel is included, the thrust is given by

$$F=M_a(V_j-V_o)+fM_aV_j \tag{1b}$$

The net thrust horsepower thp is expressed as

$$thp=FV_o/550 \tag{2}$$

The compressor-shaft horsepower is given by

$$P_c=M_aJc_{p,a}T_0Z/550=5675\ M_aZT_0/519 \tag{3}$$

The compressor-inlet total temperature is obtained from

$$T_1/T_0=1+Y \tag{4}$$

The fuel consumption per unit mass rate of air flow is given in terms of the fuel-air ratio by the following relation:

$$W_f/M_a=115{,}920\,f \tag{5}$$

DISCUSSION OF CHARTS

By means of equations (1) to (5) and the curves of figures 2 to 7, the performance of the turbojet engine can be readily determined. The curves are given in a form that shows the effects of the variables on performance. In figures 2 to 4 are shown curves for evaluating some of the primary parameters that are used in the principal performance chart, figure 5 (a), from which the jet velocity is determined. The fuel-air ratio is evaluated with the use of figures 6 and 7.

Curves for obtaining the flight Mach number, the values of Y, and the compressor-inlet total pressure for various values of the factor $V_o\sqrt{519/T_0}$ are shown in figure 2. The compressor-inlet total temperature is obtained from the value of Y and equation (4).

The value of ϵ, which accounts for the effect of the secondary group of variables, is obtained from figure 3. The quantity ϵ is given by the relation

$$\epsilon=1-a-b+c$$

Factor a, which gives the effect of total-pressure drop through the inlet duct Δp_d, is shown in figure 3 (a). Factor b, which measures the effect of total-pressure drop through the combustion chamber Δp_2, is introduced in figure 3 (b). Factor c, which corrects for the difference between the physical properties of the hot exhaust gases and the cold air involved in the computation of the expansion processes through the turbine and the exhaust nozzle, is given in figure 3 (c). In general, the value of ϵ is close to unity and can be taken as equal to unity when a rapid approximation is desired. In some cases, a change in ϵ of 1 percent may, however, introduce a change of several percent in the thrust.

The compressor total-pressure ratio is plotted against the quantity $\eta_cZ/(1+Y)$ in figure 4. The compressor-shaft horsepower (and hence the turbine-shaft horsepower) is computed from equation (3) and the value of Z. The effect of the variation in specific heat of air during compression is neglected in this plot, the maximum error in Z introduced being about 1 percent for the range of compressor pressure ratios shown in figure 4 and for compressor-inlet temperatures up to 550° R.

The value of $(p_2/p_1)_{ref}$ plotted against the factor $\eta_c\eta_t\epsilon\,\frac{T_4}{T_0}\left(\frac{1}{1+Y}\right)^2$ is also given in figure 4. The quantity $(p_2/p_1)_{ref}$ is useful in that it is the compressor pressure ratio for maximum thrust per unit mass rate of air flow for any given values of $\eta_c\eta_t\epsilon\,\frac{T_4}{T_0}$ and Y, provided that the change in ϵ with

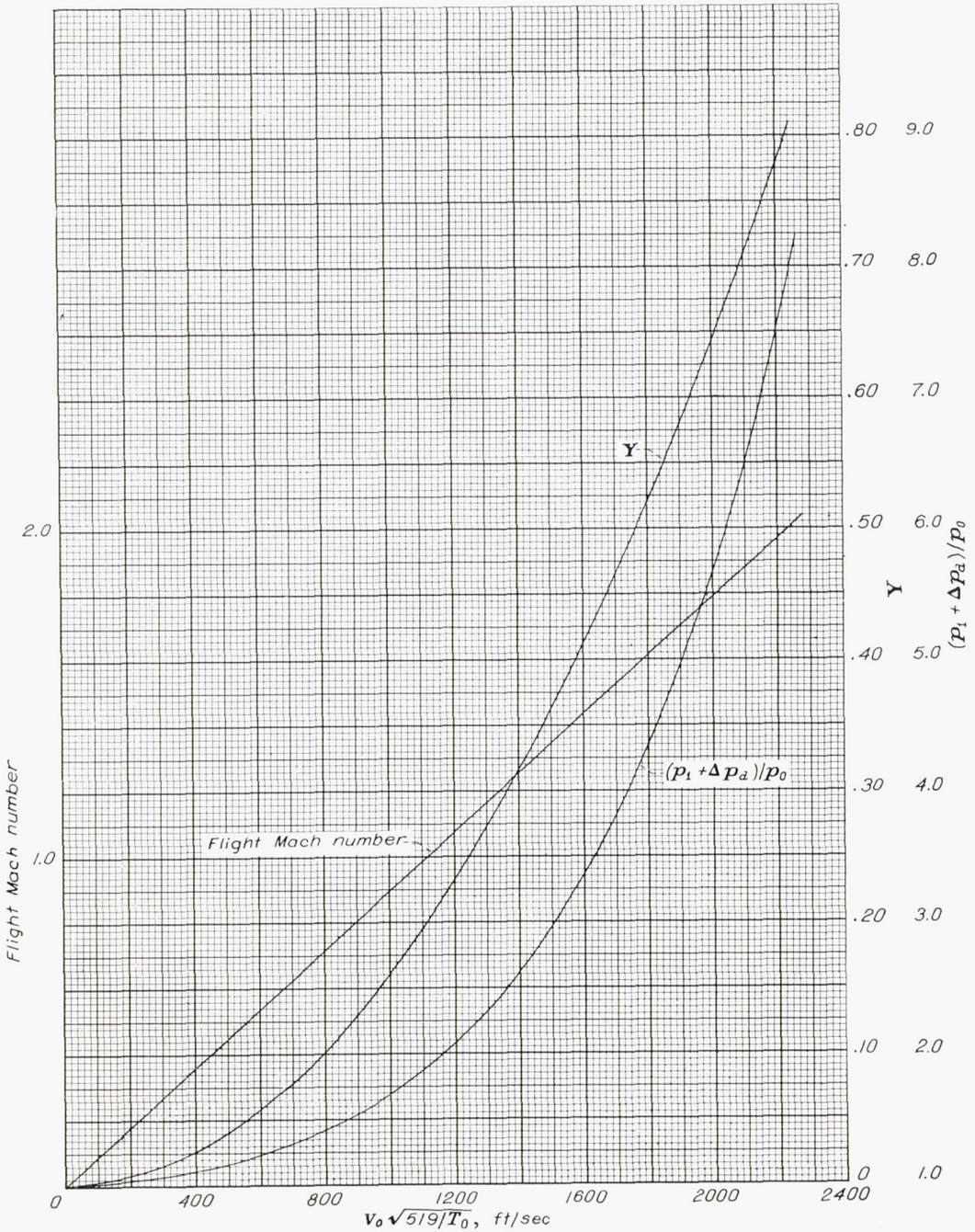
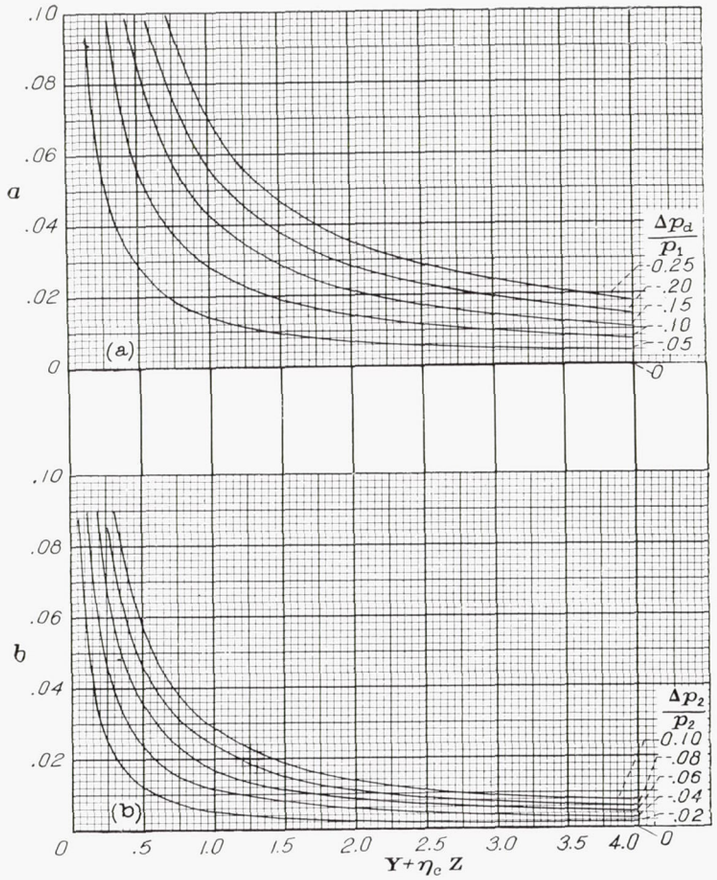
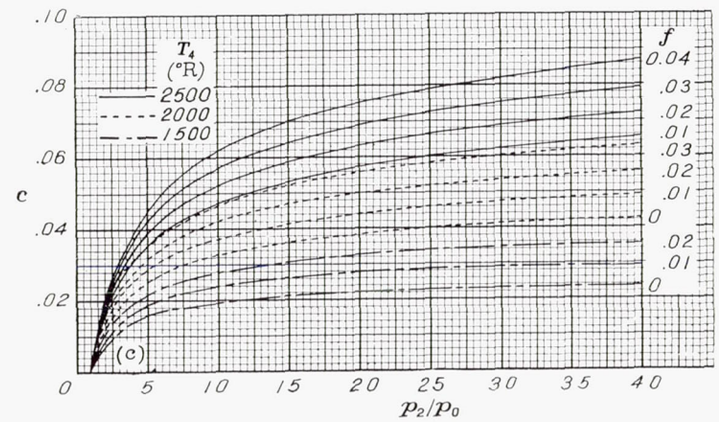


FIGURE 2.—Chart for determining flight Mach number, Y, and compressor-inlet total pressure for various airplane velocities and ambient temperatures.





(a) Correction a.
(b) Correction b.
(c) Correction c.

FIGURE 3.—Chart for determining factor ϵ. $(\epsilon=1-a-b+c)$

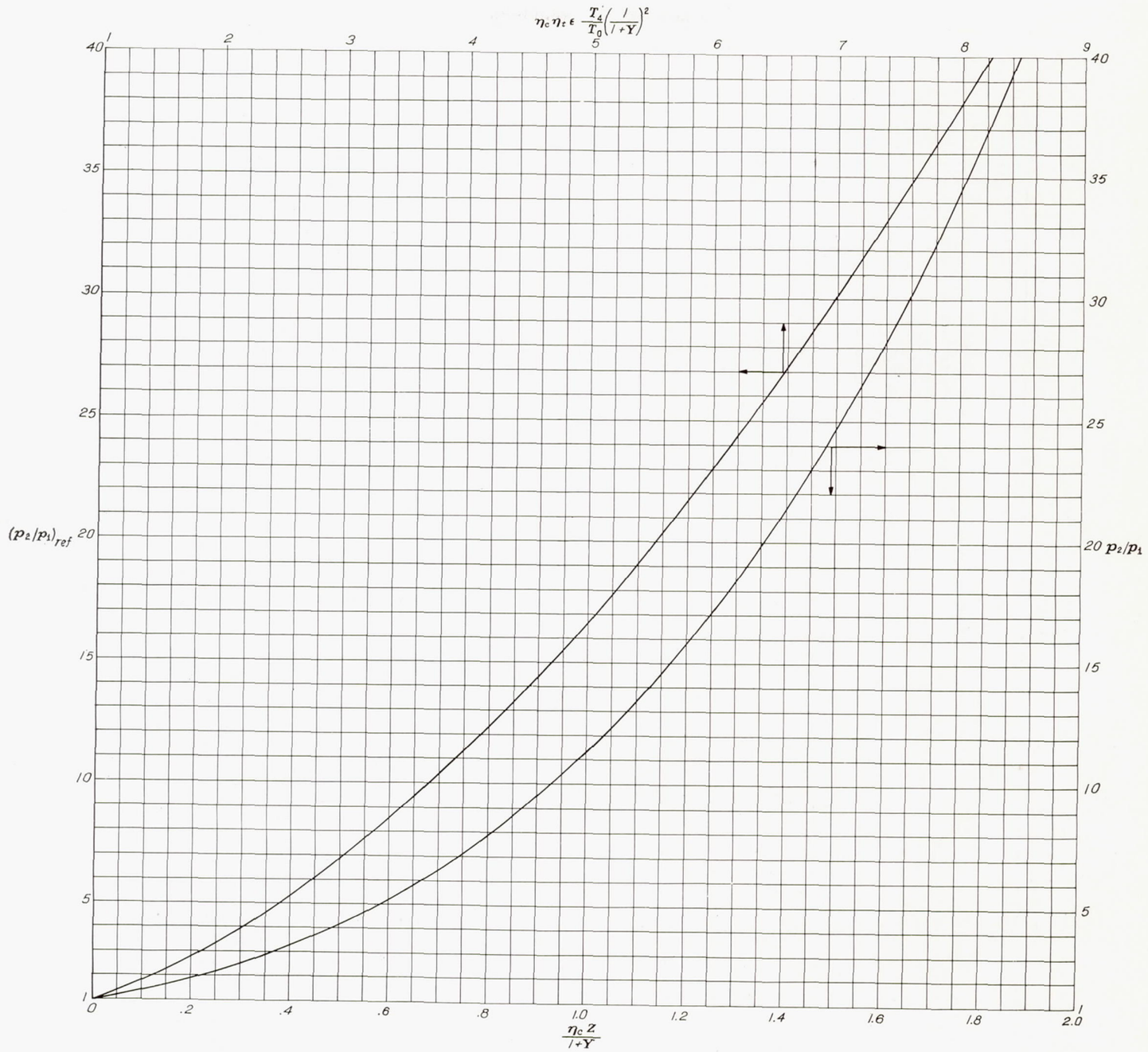
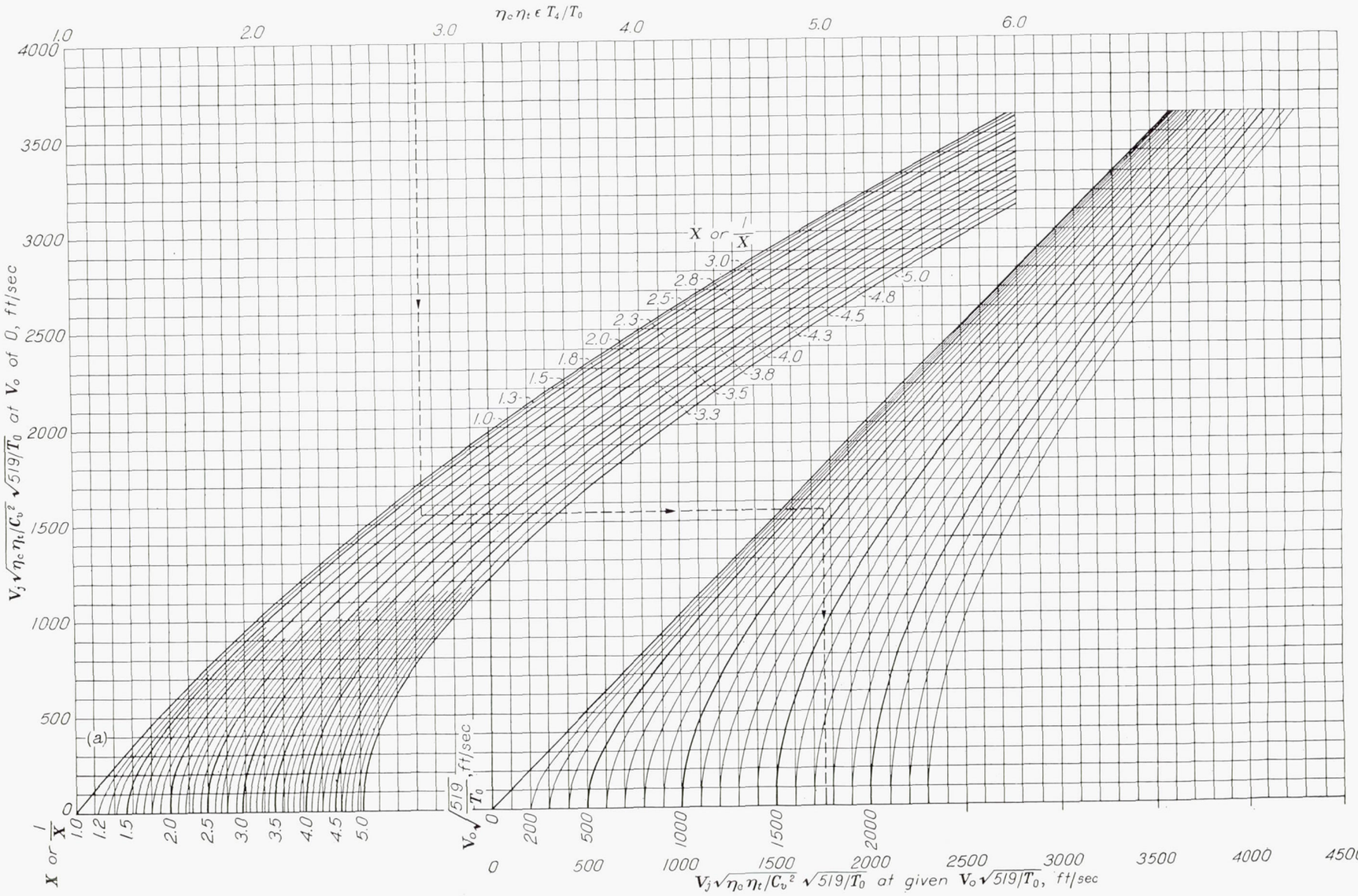


FIGURE 4.—Chart for determining reference compressor pressure ratio $(p_2/p_1)_{ref}$ for various values of $\eta_c \eta_t \epsilon \frac{T_4}{T_0}\left(\frac{1}{1+Y}\right)^2$ and for determining $\frac{\eta_c Z}{1+Y}$ for various values of compressor pressure ratio p_2/p_1.

(A 24-in. by 24-in. print of this chart is available upon request from NACA.)

change in pressure ratio is negligible. In a system where the pressure losses are low, the value of ϵ is close to and generally slightly greater than unity and varies inappreciably with p_2/p_1. When the change in ϵ with p_2/p_1 is appreciable, then $(p_2/p_1)_{ref}$ differs slightly from the compressor pressure ratio giving maximum thrust per unit mass rate of air flow. Even in this case, however, the thrust per unit mass rate of air flow corresponding to $(p_2/p_1)_{ref}$ is generally within 1 percent of the true maximum. Hence, figure 4 permits a rapid approximation of the pressure ratio for maximum thrust per unit mass rate of air flow. The actual compressor pressure ratio p_2/p_1 divided by the quantity $(p_2/p_1)_{ref}$ defines the value of X used in figure 5 (a).

The curves in figure 5 (a) are used to determine the jet-velocity factor $V_j\sqrt{\frac{\eta_c \eta_t}{C_v^2}}\sqrt{\frac{519}{T_0}}$ for various values of the parameters $\eta_c \eta_t \epsilon \frac{T_4}{T_0}$, $V_o\sqrt{519/T_0}$, and X or $1/X$. When X is less than unity, the value of $1/X$ is used because X occurs in equation (B43) (appendix A) for figure 5 (a) only in the quantity $(X)^{\frac{\gamma_a-1}{\gamma_a}}+\left(\frac{1}{X}\right)^{\frac{\gamma_a-1}{\gamma_a}}$. Corresponding to the values of $\eta_c \eta_t \epsilon \frac{T_4}{T_0}$ and X or $1/X$, a point on the left-hand set of curves is determined; then progressing horizontally across the chart



(a) Effect of turbine-loss reheat in further expansion from turbine-outlet static pressure to ambient pressure is neglected.

FIGURE 5.—Chart for determining jet velocity.

(This chart has been divided into two sections, 18 in. by 41 in. and 20 in. by 41 in., and is available upon request from NACA.)

to the desired $V_o\sqrt{519/T_0}$ line, a second point is located on the right-hand set of curves. The value of the jet-velocity factor $V_j\sqrt{\frac{\eta_c\eta_t}{C_v^2}}\sqrt{\frac{519}{T_0}}$ is read as the value of the lower abscissa of the second point. At zero flight speed, the jet-velocity factor is read directly as the ordinate of the first point located on the left-hand set of curves. The thrust can then be computed from the value of V_j and equation (1a). As previously mentioned, the value of X is found by dividing the compressor pressure ratio p_2/p_1 by the value of $(p_2/p_1)_{ref}$ obtained from figure 4 corresponding to the values of the parameters η_c, η_t, ϵ, T_4, T_0, and Y being considered.

In figure 5 (a) for given values of η_c, η_t, T_4, T_0, and Y, if ϵ remains constant as p_2/p_1 (or X) varies, then the variation of V_j with p_2/p_1 occurs along a constant $\eta_c\eta_t\epsilon\frac{T_4}{T_0}$ line. For this case $(p_2/p_1)_{ref}$, which is a function of ϵ, remains constant and the maximum value of V_j occurs at a value of p_2/p_1 equal to $(p_2/p_1)_{ref}$. Actually, however, as p_2/p_1 varies, the value of ϵ changes slightly and hence $\eta_c\eta_t\epsilon\frac{T_4}{T_0}$ changes, with the result that the variation in V_j with p_2/p_1 does not occur along a constant $\eta_c\eta_t\epsilon\frac{T_4}{T_0}$ line. Also $(p_2/p_1)_{ref}$ is no longer constant as p_2/p_1 varies and the value of X at any given p_2/p_1 must be evaluated using the $(p_2/p_1)_{ref}$ value determined at the given p_2/p_1. For this case of varying ϵ, the value of $(p_2/p_1)_{ref}$ evaluated at any p_2/p_1 is a close approximation to the p_2/p_1 giving maximum V_j.

For a case in which η_c varies with p_2/p_1, similar considerations apply as for the case of ϵ varying with p_2/p_1.

As an example of the use of figures 2, 4, and 5 (a) for a rapid approximate computation of the thrust per unit mass rate of air flow F/M_a, a case is considered in which the following conditions are given:

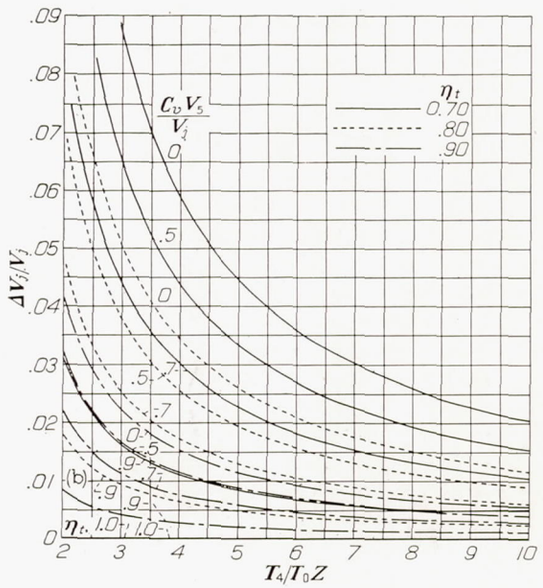
Exhaust-nozzle velocity coefficient, C_v	0.95
Compressor adiabatic efficiency, η_c	0.85
Turbine total efficiency, η_t	0.90
Turbine-inlet temperature, T_4, °R	2000
Ambient-air temperature, T_0, °R	500
Airplane velocity, V_o, ft/sec	733
Compressor pressure ratio, p_2/p_1	4

From the assumption that ϵ is equal to 1, F/M_a is then evaluated using these given quantities as follows:

$V_o\sqrt{519/T_0}$, ft/sec	747
Y (from fig. 2)	0.089
$\eta_c\eta_t\epsilon\frac{T_4}{T_0}$	3.06
$\eta_c\eta_t\epsilon\frac{T_4}{T_0}\left(\frac{1}{1+Y}\right)^2$	2.58
$(p_2/p_1)_{ref}$ (from fig. 4)	5.25
$1/X=(p_2/p_1)_{ref}/(p_2/p_1)$	1.31
$V_j\sqrt{\frac{\eta_c\eta_t}{C_v^2}}\sqrt{\frac{519}{T_0}}$ (from fig. 5(a)), ft/sec	2000
V_j, ft/sec	2132
F/M_a (from equation (1a)), lb/(slug/sec)	1399

Subsequent charts and discussion introduce corrections that permit a high degree of accuracy when desired.

The losses in kinetic energy in the turbine passages appear as heat energy in the gas leaving the turbine. This energy will be termed "turbine-loss reheat." In the further expansion of the gas in passing through the exhaust nozzle, some of the turbine-loss reheat is recovered as additional kinetic energy of the jet. If, however, the velocity at the turbine outlet is substantially equal to the final jet velocity, no further expansion occurs and no kinetic energy is recovered from the turbine-loss reheat. The curves of figure 5 (a) correspond to this case. The ratio of the increase in jet velocity to the final jet velocity $\Delta V_j/V_j$ (V_j determined from fig. 5 (a)), obtained when the velocity at the turbine outlet V_5 is less than the final jet velocity, is shown in figure 5 (b). The curves presented in this figure are based on a value of specific heat at constant pressure for exhaust gas equal to 8.9 Btu per slug per °F.



(b) Correction to jet velocity due to reheat in turbine. ($c_{p,a}$, 8.9 Btu/(slug)(°F))

FIGURE 5.—Concluded. Chart for determining jet velocity.

When C_vV_5/V_j is 1, then for all values of turbine total efficiency $\Delta V_j/V_j$ is 0 (fig. 5 (b)). Also, $\Delta V_j/V_j$ approaches 0 as turbine total efficiency approaches 1 for all values of C_vV_5/V_j because turbine-loss reheat approaches 0 with increase in turbine total efficiency.

For a given turbine total efficiency, the smaller the value of C_vV_5/V_j, the greater is the recovery of turbine-loss reheat as is evident from figure 5 (b). Decrease in turbine-outlet velocity V_5 is obtained by an increase in annular area swept by the turbine blades. Blade stress is one of the principal limitations on blade height and thus on blade-annulus area.

The compressor-outlet total temperature T_2 plotted against the factor $T_0(1+Y+Z)$ is shown in figure 6. This curve includes the variation in specific heat of air during compression and was computed using reference 6. The variation in specific heat is accounted for in this case, whereas it is neglected in figure 4 because the error introduced in the evaluation of the temperature rise during compression by the assumption of a constant value of specific heat is much greater than the error introduced by the same assumption in the evaluation of the compressor power.

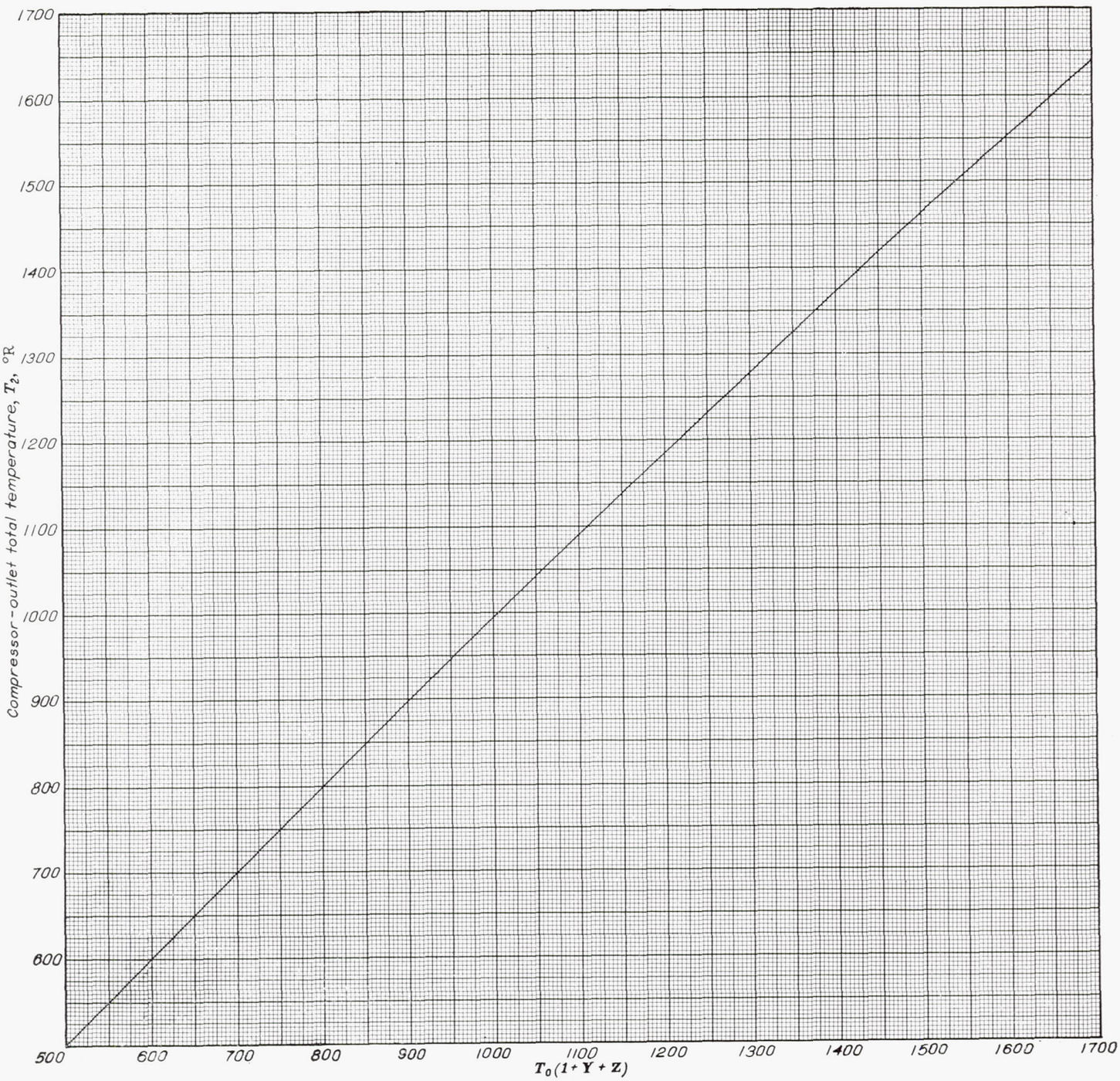


FIGURE 6.—Chart for determining compressor-outlet total temperature for various values of the factor $T_0(1+Y+Z)$.

The fuel-air-ratio factor $\eta_b f$ is plotted in figure 7 against $T_4 - T_2$ (total-temperature rise in combustion chamber) for various values of T_4. These curves were based on the latest available information on specific heats of air and exhaust-gas mixtures (reference 7) and are for a fuel having a lower heating value h of 18,900 Btu per pound and a hydrogen-carbon ratio of 0.185. For fuels having other values of h, the value of f given in figure 7 is corrected accurately by multiplying it by the factor $18{,}900/h$. The effect of hydrogen-carbon ratio of fuel on f is generally small, and for a range of hydrogen-carbon ratios from 0.16 to 0.21, the error due to the deviation from the value of 0.185 is less than one-half of 1 percent. The fuel consumption per unit mass rate of air flow is obtained from the value of f and equation (5).

In the preceding discussion of the charts, the effect of the mass of injected fuel was not mentioned. It is shown in appendix B that the effect of the added fuel on the jet velocity can be taken into account by substituting the product of turbine total efficiency η_t and $(1+f)$ for the value of η_t in the charts. This adjustment occurs in figure 4 in the factor $\eta_c\eta_t\epsilon \dfrac{T_4}{T_0}\left(\dfrac{1}{1+Y}\right)^2$, which is used in finding $(p_2/p_1)_{ref}$, and in the factors $\eta_c\eta_t\epsilon \dfrac{T_4}{T_0}$ and $V_j\sqrt{\dfrac{\eta_c\eta_t}{C_v^2}}\sqrt{\dfrac{519}{T_0}}$ of figure 5 (a). The value of V_j determined is then used in equation (1b), which includes effect of added fuel.

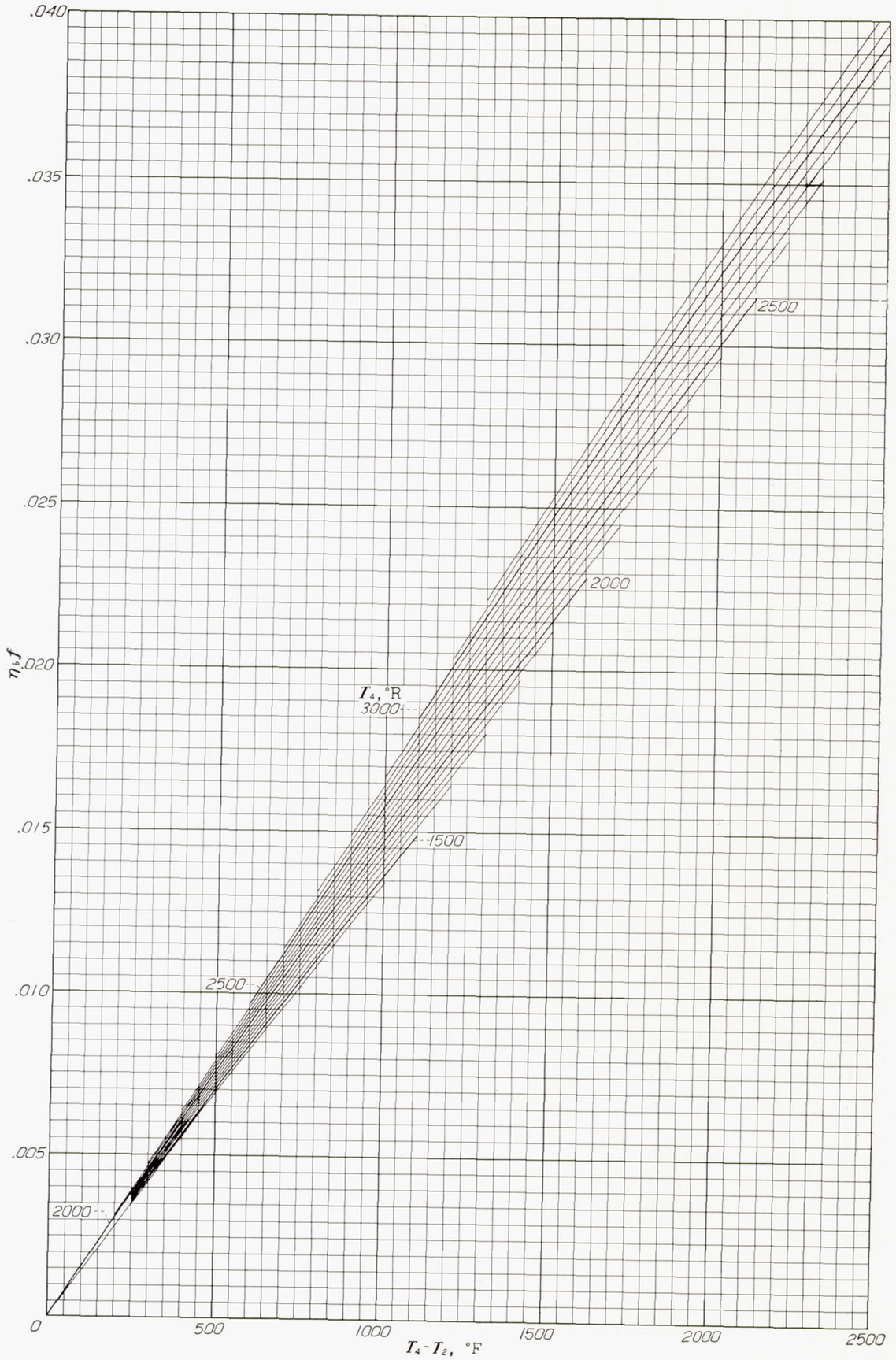


FIGURE 7.—Chart for determining fuel-air ratio for various values of rise in total temperature through combustion chamber and values of combustion-chamber-outlet total temperature. (h, 18,900 Btu/lb)

(A 23-in. by 35-in. print of this chart is available upon request from NACA.)

EXAMPLE OF USE OF CHARTS

The use of figures 2 to 7 in evaluating such performance values as compressor-shaft horsepower, fuel consumption, jet velocity, thrust per unit mass rate of air flow, thrust horsepower, and specific fuel consumption is illustrated in the following example. The method of accounting for added fuel mass and turbine-loss reheat is also shown. The example is based on a system having the following engine and flight operating conditions:

1. Compressor adiabatic efficiency, η_c	0. 80
2. Turbine total efficiency, η_t	0. 90
3. Combustion efficiency, η_b	0. 97
4. Exhaust-nozzle velocity coefficient, C_v	0. 96
5. Airplane velocity, V_o, ft/sec	733
6. Compressor total-pressure ratio, p_2/p_1	6
7. Ambient-air pressure, p_0, in. Hg	29. 9
8. Ambient-air temperature, T_0, °R	519
9. Combustion-chamber-outlet total temperature, T_4, °R	1960
10. Total-pressure drop through inlet duct, Δp_d, in. Hg	0. 5
11. Total-pressure drop through combustion chamber, Δp_2, in. Hg	3
12. Lower heating value of fuel, h, Btu/lb	18, 500

Determination of Y and flight Mach number

From items 5 and 8	
13. $V_o\sqrt{519/T_0}$, ft/sec	733
From item 13 and figure 2	
14. Y	0. 0861
15. Flight Mach number	0. 656

Determination of Z and P_c

Item 6 read on figure 4 determines	
16. $\frac{\eta_c Z}{1+Y}$	0.669
From items 16, 14, and 1	
17. Z	0. 908
Using items 17 and 8 in equation (3) gives the compressor-shaft horsepower per unit mass rate of air flow	
18. P_c/M_a, hp/(slug/sec)	5153

Determination of f and W_f/M_a

From items 8, 14, and 17	
19. $T_0(1+Y+Z)$, °R	1035
Using item 19 and figure 6	
20. T_2, °R	1025
From items 20 and 9	
21. T_4-T_2, °F	935
From items 21, 9, and figure 7	
22. $\eta_b f$	0. 01372
Items 22 and 3 give	
23. f	0. 01414
Because the lower heating value of the fuel is equal to 18,500 Btu per pound (item 12), item 23 has to be multiplied by the factor $\frac{18{,}900}{18{,}500}$ and the adjusted value is	
24. f	0. 01445
From item 24 and equation (5)	
25. W_f/M_a, (lb/hr)/(slug/sec)	1675

Determination of factor ϵ

From items 7, 10, and 11	
26. $\Delta p_d/p_0$	0. 017
27. $\Delta p_2/p_0$	0. 10
From figure 2 and item 13	
28. $\frac{p_1+\Delta p_d}{p_0}$	1. 335
and using item 26 with item 28 gives	
29. p_1/p_0	1. 318
Using items 29 and 6	
30. p_2/p_0	7. 91
From items 26 and 29	
31. $\Delta p_d/p_1$	0. 013
whereas from items 27 and 30	
32. $\Delta p_2/p_2$	0. 013
From items 14 and 16	
33. $Y+\eta_c Z$	0. 812
Items 31 and 33 in figure 3 (a) give	
34. a	0. 005
Using items 32 and 33 in figure 3 (b) gives	
35. b	0. 005
When items 9, 24, and 30 are used in figure 3 (c)	
36. c	0. 035
From items 34, 35, and 36	
37. $\epsilon=1-0.005-0.005+0.035$	1. 025

Determination of $(p_2/p_1)_{ref}$ and X

Using items 1, 2, 37, 9, 8, and 14 gives	
38. $\eta_c\eta_t\epsilon\frac{T_4}{T_0}\left(\frac{1}{1+Y}\right)^2$	2. 363
From item 38 and figure 4	
39. $(p_2/p_1)_{ref}$	4. 50
From items 6, 39, and the definition of parameter X	
40. X	1. 333

Determination of V_j, F/M_a, and other performance parameters when effects of added fuel and of turbine-loss reheat are neglected

Using items 1, 2, 37, 9, and 8 gives	
41. $\eta_c\eta_t\epsilon\frac{T_4}{T_0}$	2. 787
From items 41, 40, 13, and figure 5 (a), the jet-velocity factor is	
42. $V_j\sqrt{\frac{\eta_c\eta_t}{C_v^2}}\sqrt{\frac{519}{T_0}}$, ft/sec	1806
and from items 42, 1, 2, 4, and 8	
43. V_j, ft/sec	2044
The net thrust per unit mass rate of air flow is obtained from items 43, 5, and equation (1a)	
44. F/M_a, lb/(slug/sec)	1311
The thrust horsepower per unit mass rate of air flow is calculated from items 44, 5, and equation (2)	
45. thp/M_a, thp/(slug/sec)	1747
From items 25 and 44	
46. W_f/F, (lb/hr)/lb thrust	1. 278
and from items 25 and 45	
47. W_f/thp, lb/thp-hr	0. 959

Effect of mass of added fuel and of turbine-loss reheat on V_j and F/M_a

When more accurate results are desired, the calculations are made taking into account the effect of the mass of fuel introduced and the effect of turbine-loss reheat. The effect of the fuel on jet velocity is handled by substituting the product of the turbine total efficiency η_t and $(1+f)$ for the value of η_t, which will now be done for the case just considered.

From items 24 and 38	
48. $\eta_c\eta_t\epsilon\frac{T_4}{T_0}\left(\frac{1}{1+Y}\right)^2$	2.396
From figure 4 the corresponding	
49. $(p_2/p_1)_{ref}$	4.61
From items 6 and 49	
50. X	1.30
Similarly with the effect of fuel flow included, item 41 becomes	
51. $\eta_c\eta_t\epsilon\frac{T_4}{T_0}$	2.827
so that from items 50, 51, 13, and figure 5 (a)	
52. $V_j\sqrt{\frac{\eta_c\eta_t}{C_v^2}}\sqrt{\frac{519}{T_0}}$, ft/sec	1832

Again in order to account for the effect of fuel by an adjustment of the η_t term

53. V_j, ft/sec 2065

which differs from item 43 by 1 percent.

The effect of turbine-loss reheat may be important when η_t is considerably less than unity and the velocity at the turbine outlet is appreciably less than the final jet velocity. In the example being discussed, the assumption is made that the turbine is designed to have an outlet velocity

54. V_5, ft/sec 700

Then from items 4, 53, and 54

55. $C_v V_5/V_j$ 0. 33

From items 8, 9, and 17

56. $\frac{T_4}{T_0 Z}$ 4.16

Using items 2, 55, and 56 in figure 5 (b) gives

57. $\Delta V_j/V_j$ 0. 012

and from items 53 and 57

58. ΔV_j, ft/sec 25

Using items 58 and 53 gives

59. Corrected V_j, ft/sec 2090

Thus in this case, turbine-loss reheat provides an additional 1-percent increase in the value of V_j.

The thrust per unit mass rate of air flow is obtained from items 59, 5, and equation (1b) as

60. F/M_a, lb/(slug/sec) 1357

which is comparable with a value of 1311 (item 44) in which the effects of fuel and reheat were neglected.

From equation (2) and items 60 and 5

61. thp/M_a, thp/(slug/sec) 1808

and using items 25 and 60 gives

62. W_f/F, (lb/hr)/lb 1. 234

and items 25 and 61 give

63. W_f/thp, lb/thp-hr 0. 926

TURBOJET-ENGINE PERFORMANCE

In order to illustrate the performance and some of the characteristics of the turbojet engine, several cases are presented. First, the characteristics of a turbojet system operating with fixed component efficiencies over a range of flight and engine operating conditions are discussed. These characteristics pertain to a series of turbojet engines whose design-point conditions at any operating point are equal to the given conditions at that operating point. Second, the characteristics of a turbojet engine with a given set of matched components operating over a range of flight and engine operating conditions are discussed. For this case a method of matching components and determining the interrelation between component characteristics and their effect on over-all engine performance, as operating conditions vary, is presented.

DESIGN-POINT ENGINES

For the purpose of illustrating the manner in which the thrust per unit mass rate of air flow and the specific fuel consumption are influenced by compressor pressure ratio, combustion-chamber-outlet temperature, flight speed, and ambient-air temperature, the following fixed parameters are assumed:

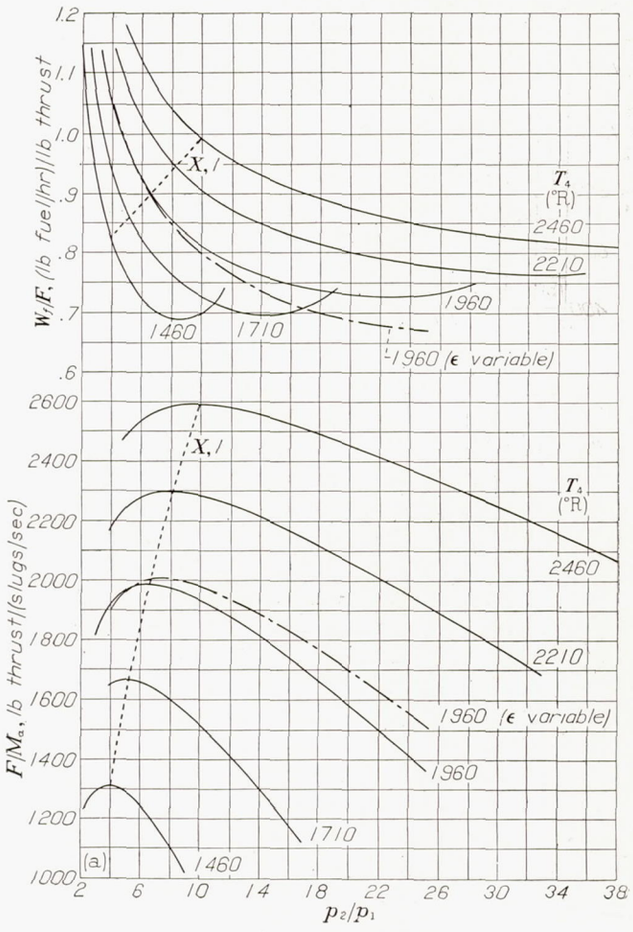
Compressor adiabatic efficiency, η_c	0. 85
Turbine total efficiency, η_t	0. 90
Combustion efficiency, η_b	0. 96
Exhaust-nozzle velocity coefficient, C_v	0. 97
Lower heating value of fuel, h, Btu/lb	18, 900
Correction factor, ϵ	1. 00

These compressor and turbine efficiencies are not unreasonably high when it is considered that in the definition of these efficiencies the compressor and the turbine are credited with the kinetic energy of the gases at the compressor and turbine outlets, respectively.

The computed turbojet performance in this illustrative case includes the effect of the mass of added fuel.

The values of component efficiencies and ϵ for any given turbojet engine vary with altitude and flight speed. In the present computations, the component efficiencies and ϵ were assumed constant at the values listed. Computations were also made for a case in which the variation of ϵ with compressor pressure ratio is considered.

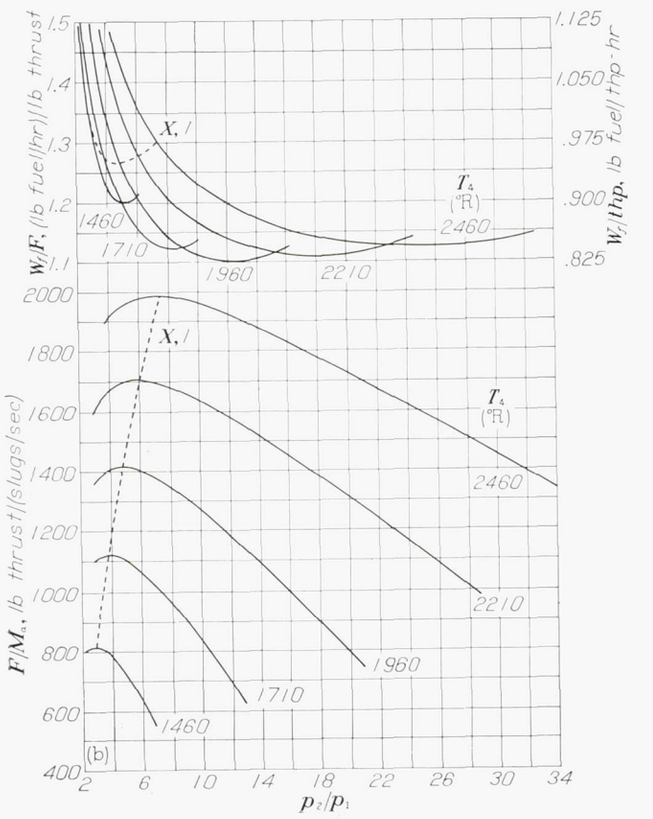
The specific fuel consumption and the thrust per unit mass rate of air flow plotted against the compressor pressure ratio for various values of combustion-chamber-outlet temperature are shown in figure 8 for several combinations of ambient temperature and airplane velocity. A line for compressor pressure ratios giving maximum thrust per unit mass rate of air flow ($X=1$) is also included in the figure. Figure 8 (a),

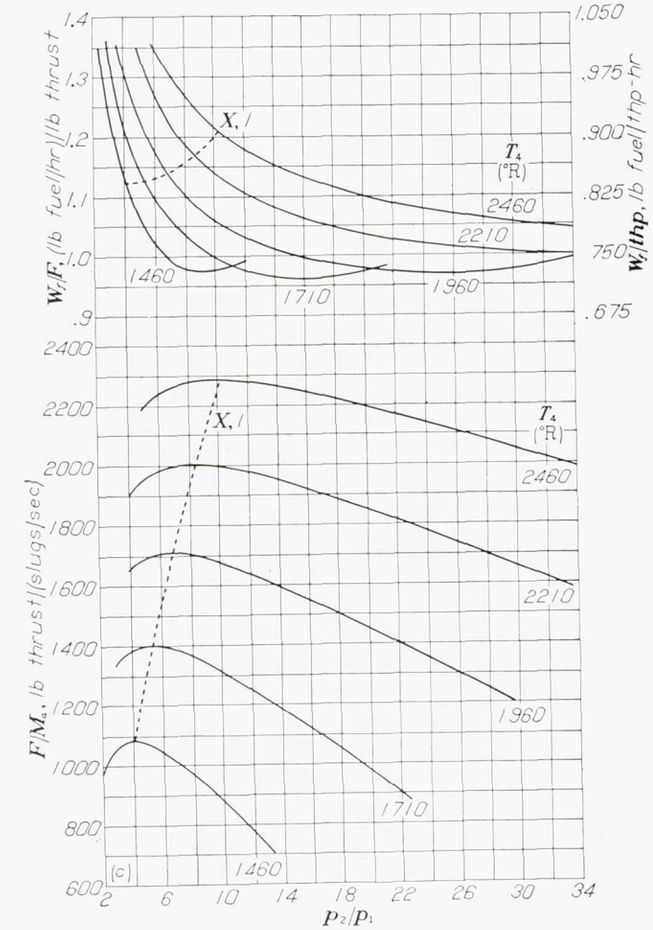


(a) V_o, 0 feet per second; T_0, 519° R.

FIGURE 8.—Specific fuel consumption and thrust per unit mass rate of air flow for various compressor pressure ratios and combustion-chamber-outlet temperatures for illustrative case. (η_c, 0.85; η_t, 0.90; η_b, 0.96; C_v, 0.97; h, 18,900 Btu/lb; ϵ, 1.00)

which is for V_o of 0 feet per second and T_0 of 519° R, includes a curve for T_4 of 1960° R where the variation in ϵ with p_2/p_1 is considered. For this curve, constant values of $\Delta p_d/p_1$ of 0.03 and $\Delta p_2/p_2$ of 0.04 were chosen because these values give a value of ϵ of 1.00 at a pressure ratio of about 5.6. At pressure ratios greater than 5.6, the values of ϵ are greater than 1.00. The value of compressor pressure ratio for a maximum value of F/M_a is greater for the case where ϵ varies with pressure ratio than for the case where ϵ is assumed constant, and the peak value of F/M_a for the first case is slightly greater than that for the second case (fig. 8 (a)).





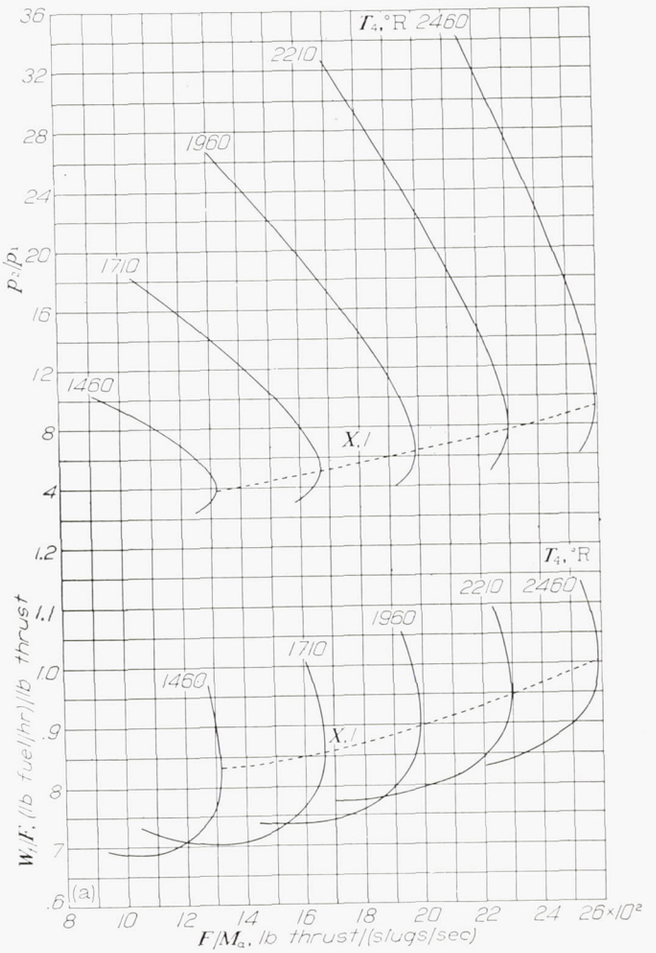
(b) V_o, 733 feet per second; T_0, 519° R.
(c) V_o, 733 feet per second; T_0, 412° R.

FIGURE 8.—Concluded.

The compressor pressure ratio and specific fuel consumption plotted against thrust per unit mass rate of air flow in figure 9 is a replot of figure 8. A scale of the power specific fuel consumption in pounds per thrust horsepower-hour is added on figures 8 (b) and 9 (b), which are for V_o of 733 feet per second and T_0 of 519° R, and on figures 8 (c) and 9 (c), which are for V_o of 733 feet per second and T_0 of 412° R.

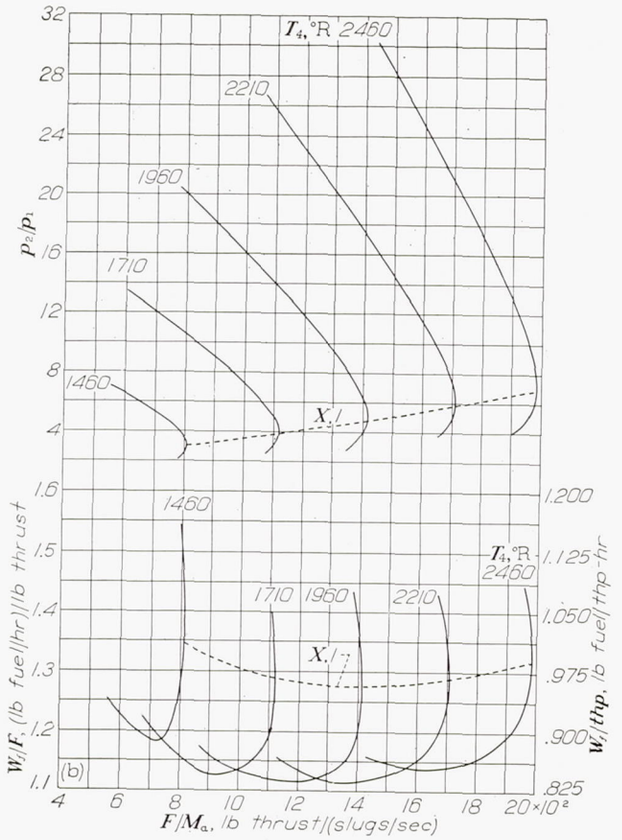
It is illustrated in figures 8 and 9 that the minimum specific fuel consumption occurs at a higher compressor pressure ratio than maximum thrust per unit mass rate of air flow. When high thrust per unit mass rate of air flow rather than low specific fuel consumption is the primary consideration, it is apparent from figures 8 and 9 that high combustion-chamber-outlet temperatures should be used. High thrust is the more important consideration in take-off, climb, and maximum-speed operation.

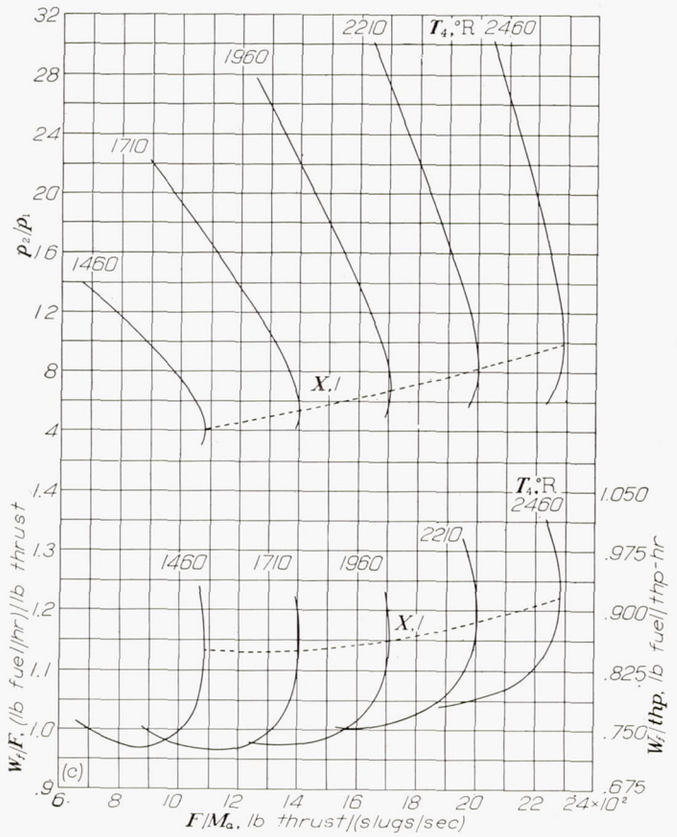
The curves of figure 9 show that with no limitation on the compressor pressure ratio, as the combustion-chamber-outlet temperature is increased from the minimum value required to produce a thrust, the thrust per unit mass rate of air flow increases and the specific fuel consumption decreases until the temperature giving minimum specific fuel consumption is reached. Increasing the temperature further results in both increased thrust per unit mass rate of air flow and specific fuel consumption. This temperature for minimum specific fuel consumption is less than 1460° R for figure 9 (a),



(a) V_o, 0 feet per second; T_0, 519° R.

FIGURE 9.—Compressor pressure ratio and specific fuel consumption for various thrusts per unit mass rate of air flow and combustion-chamber-outlet temperatures for illustrative case. (η_c, 0.85; η_i, 0.90; η_b, 0.96; C_s, 0.97; h, 18,900 Btu/lb; ϵ, 1.00)





(b) V_o, 733 feet per second; T_b, 519° R.
(c) V_o, 733 feet per second; T_b, 412° R.

FIGURE 9.—Concluded.

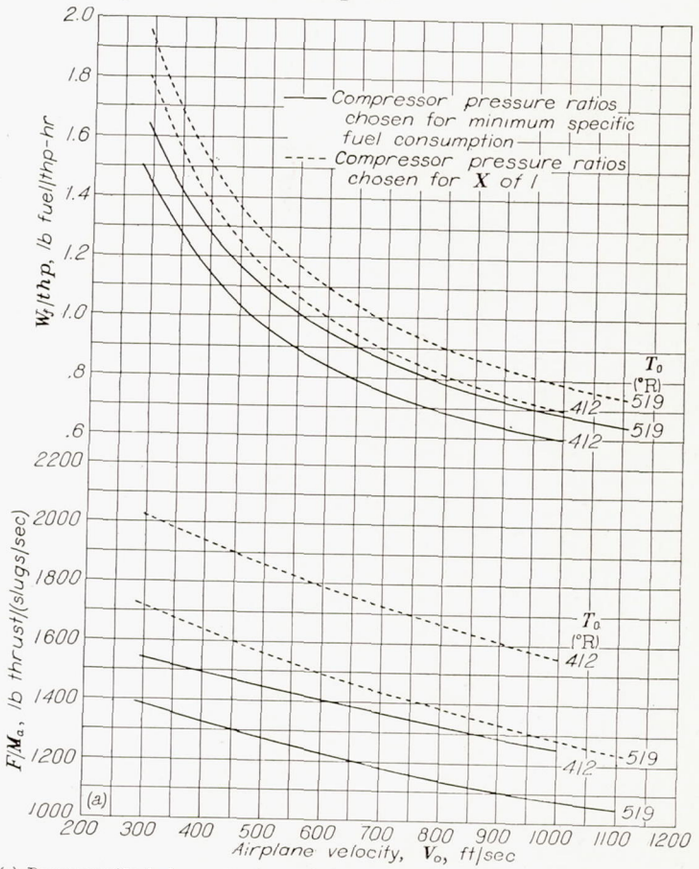
about 2210° R for figure 9 (b), and 1710° R for figure 9 (c), indicating that at some conditions the temperature for minimum specific fuel consumption is less than the temperature limit imposed by strength-temperature characteristics of turbine materials.

If the available compressor pressure ratio is limited, the combustion-chamber-outlet temperature for minimum specific fuel consumption is sensitive to the other operating conditions. For example, at a limiting compressor pressure ratio of 4, minimum specific fuel consumption occurs at a temperature below the lowest values shown in figure 8. If the limiting compressor pressure ratio is 8, the combustion-chamber-outlet temperature for minimum specific fuel consumption is just slightly less than the lowest temperature shown in figure 8 (c) for an ambient temperature of 412° R but approaches an intermediate value of approximately 1710° R for an ambient temperature of 519° R (fig. 8 (b)). Although not shown, the optimum combustion-chamber-outlet temperature is also sensitive to the efficiencies of the components of the turbojet engine.

In figure 10 (a), the power specific fuel consumption and the thrust per unit mass rate of air flow are plotted against airplane velocity at ambient temperatures of 412° and 519° R for the following cases:

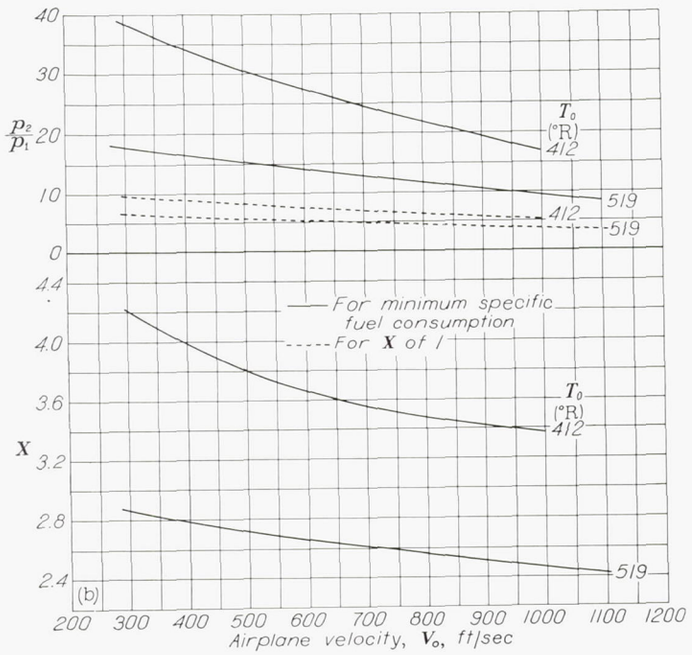
(a) Compressor pressure ratio chosen to give maximum thrust per unit mass rate of air flow ($X=1$)

(b) Compressor pressure ratio chosen to give minimum specific fuel consumption



(a) Power specific fuel consumption and thrust per unit mass rate of air flow at various airplane velocities.

FIGURE 10.—Performance at conditions for minimum specific fuel consumption and for pressure ratios giving maximum thrust per unit mass rate of air flow ($X=1$) for illustrative case. (T_4, 1960° R; η_c, 0.85; η_t, 0.90; η_b, 0.96; C_b, 0.97; h, 18,900 Btu/lb; ϵ, 1.00)



(b) Compressor pressure ratios and X at various airplane velocities.

FIGURE 10.—Concluded.

The power specific fuel consumption for case (a) is between 15 and 23 percent higher than for case (b) for airplane velocities between 300 and 800 feet per second; the percentage difference in power specific fuel consumption is greater at the lower airplane velocities and at the lower ambient temperatures.

The thrust per unit mass rate of air flow is between 21 and 31 percent higher for case (a) than for case (b) for airplane velocities between 300 and 800 feet per second; the greater percentage difference in thrust per unit mass rate of air flow occurs at the lower airplane velocities and the lower ambient temperatures.

The compressor pressure ratios and the values of X that are associated with the performance values given in figure 10 (a) are presented in figure 10 (b). The large increase in required pressure ratio from the condition of $X=1$ to the condition of minimum specific fuel consumption is noted.

In figures 8 to 10, it was assumed that the compressor adiabatic efficiency remains constant at 0.85 regardless of pressure ratio. As the desired pressure ratio is increased, however, it becomes increasingly difficult to design a compressor to maintain a high adiabatic efficiency; a reduction in compressor adiabatic efficiency may therefore be expected. The reduction in the obtainable compressor adiabatic efficiency with increase in pressure ratio reduces the gains derived from increase in pressure ratio and hence reduces the value of the optimum pressure ratio.

This condition is illustrated in figure 11 in which a turbojet engine equipped with a multistage axial-flow compressor having a polytropic efficiency $\eta_{c,p}$ of 0.88 is considered. The other parameters of the turbojet engine are the same as for figure 8 (c). Figure 11 shows the over-all adiabatic efficiency of the compressor, the thrust specific fuel consumption of the engine, and the thrust per unit mass rate of air flow plotted against pressure ratio. The pressure ratio is increased by adding stages to the compressor. Although the polytropic efficiency is held constant, the over-all compressor adiabatic efficiency decreases with increase in pressure ratio. At a pressure ratio of 5, the compressor adiabatic efficiency is 0.85, the value used in the computation for figures 8 to 10. The dashed curves on figure 11 are taken from figure 8 (c). For the range of combustion-chamber-outlet temperatures T_4 shown, the values of compressor pressure ratios for maximum F/M_a and minimum W_f/F are lower for the case when the reduction in compressor adiabatic efficiency with increased pressure ratio is considered than those for the case of constant compressor adiabatic efficiency of 0.85. This change in pressure ratios for maximum F/M_a and minimum W_f/F is more pronounced at the higher values of T_4.

The curves in figure 11 pertain to the increase in pressure ratio that is obtained by increasing the number of stages. In a turbojet engine having a given compressor, an increase in pressure ratio is obtained by an increase in rotational speed. High rotational speeds are usually accompanied by a reduction in compressor adiabatic efficiency. This case is discussed in greater detail later.

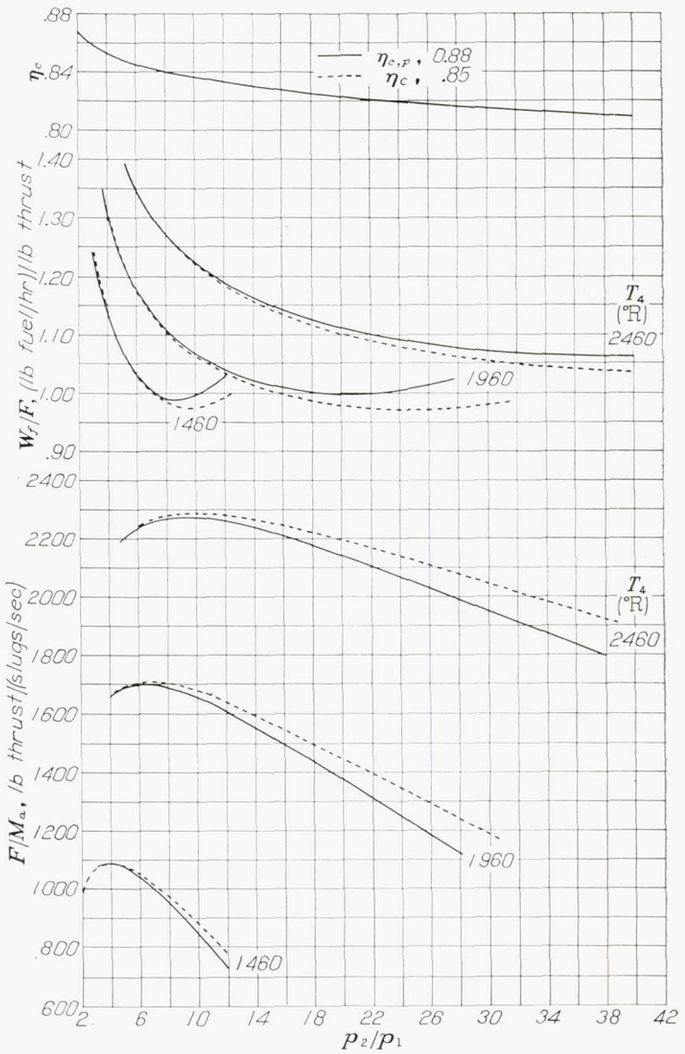


FIGURE 11.—Comparison of performance with constant η_c and with constant $\eta_{c,p}$ at various compressor pressure ratios. (V_0, 733 ft/sec; T_0, 412° R; η_t, 0.90; η_b, 0.96; C_s, 0.97; h, 18,900 Btu/lb; ϵ, 1.00)

The effect of increase in pressure ratio on turbine efficiency is a more complex matter and is not considered in detail herein. An increase in the number of turbine stages with a constant pressure ratio and efficiency per stage results in an increase in over-all turbine efficiency. There is a tendency, however, to design for increased pressure ratio per stage in addition to increasing the number of stages when increased over-all pressure ratios are desired, in order to economize on the size and the weight of the turbine. Operation at increased pressure ratio per stage may result in some reduction in turbine efficiency per stage, which may offset gains obtained from the increased number of stages. The net effect on the over-all turbine efficiency depends on the compromise between pressure ratio per stage and number of stages.

ENGINE WITH GIVEN SET OF MATCHED COMPONENTS

The points on the curves of figures 8 to 11 relate to a series of turbojet engines in which the components are changed to provide the desired characteristics at each point. It is of some interest to examine over a variety of operating conditions the characteristics of a turbojet engine having a given turbine and compressor.

The performance characteristics of the engine depend on the performance characteristics of the particular compressor, combustion chamber, and turbine chosen; the essential trends, however, may be demonstrated by a consideration of several illustrative cases. The characteristics of a typical turbine, centrifugal-flow compressor, and axial-flow compressor are shown in figures 12 to 14 followed by plots (figs. 15 and 16) of the performance characteristics of two turbojet engines incorporating these components, the first engine utilizing the centrifugal-flow compressor and the second utilizing the axial-flow compressor. The characteristics of the components discussed are purely illustrative and are not to be interpreted as indicative of the best performance obtainable. The discussion is simplified by neglecting the mass of fuel in evaluating the turbine output and by assuming the pressure drop through the combustion chamber proportional to the combustion-chamber-inlet pressure. The errors introduced by these simplifications are too small to influence the basic trends illustrated. In the computation of the performance of the turbojet engines, the following parameters are assumed:

Combustion efficiency, η_b	0.96
Exhaust-nozzle velocity coefficient, C_v	0.97
Lower heating value of fuel, h, Btu/lb	18,900

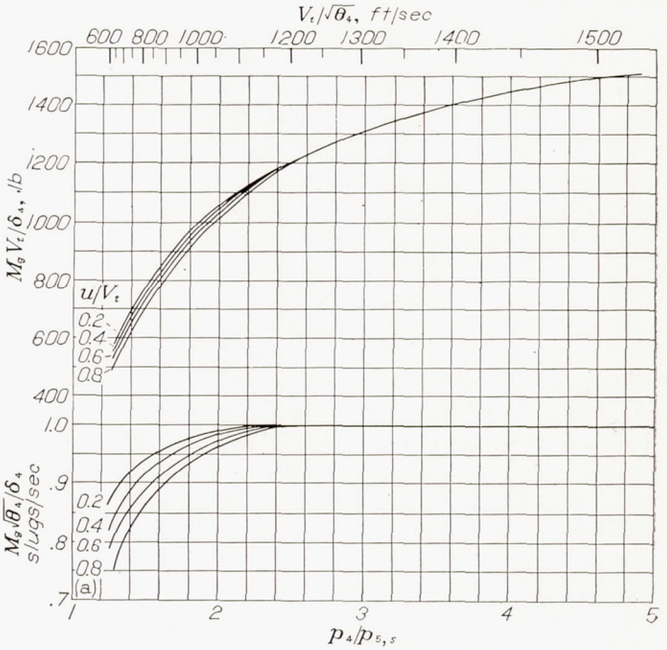
The variation in ϵ is taken into account in these calculations.

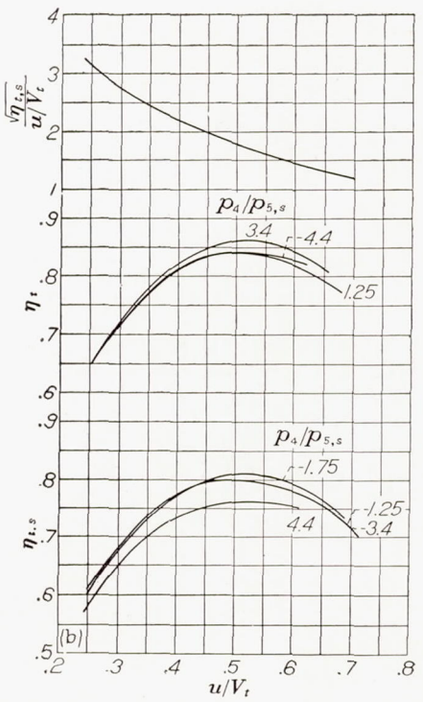
Turbine characteristics.—The performance characteristics of a typical single-stage turbine of low reaction are shown in figure 12. The mass flow of gas through the turbine is presented in figure 12 (a) by a plot of $M_g\sqrt{\theta_4}/\delta_4$ against $p_4/p_{5,s}$ at various values of the ratio of turbine-blade speed to turbine jet velocity u/V_t. The turbine jet velocity V_t is defined as the theoretical jet velocity developed by a gas expanding isentropically through the turbine nozzle from turbine-inlet total temperature and pressure to turbine-outlet static pressure. The values of the upper abscissa $V_t/\sqrt{\theta_4}$ corresponding to the values of $p_4/p_{5,s}$ are obtained from the velocity equation

$$V_t=\sqrt{2Jc_{p,g}T_4\left[1-\left(\frac{p_{5,s}}{p_4}\right)^{\frac{\gamma_g-1}{\gamma_g}}\right]}$$

The values of the upper ordinate M_gV_t/δ_4 are obtained from the product of $M_g\sqrt{\theta_4}/\delta_4$ and $V_t/\sqrt{\theta_4}$. For pressure ratios across the turbine greater than 2.5, the value of $M_g\sqrt{\theta_4}/\delta_4$ is constant (that is, choking occurs at the turbine nozzle).

The turbine total efficiency η_t is principally a function of the ratio of turbine-blade speed to turbine jet velocity u/V_t





(a) Mass-flow characteristics.
(b) Efficiency characteristics.

FIGURE 12.—Characteristics of single-stage turbine.

and to a lesser extent a function of the pressure ratio and Reynolds number. The relation between total efficiency, blade-to-jet speed ratio, and pressure ratio is given in figure 12 (b), the Reynolds number effect being omitted in this analysis. The turbine-shaft efficiency $\eta_{t,s}$, also shown in figure 12 (b), is defined as

$$\eta_{t,s}=\frac{550\,P_t}{\frac{1}{2}M_gV_t^2} \tag{6}$$

In this definition the turbine is not credited with the kinetic power corresponding to the average axial velocity of the gas at the turbine outlet. In the plot of $\frac{\sqrt{\eta_{t,s}}}{u/V_t}$ against u/V_t in figure 12 (b), the effect of $p_4/p_{5,s}$ is so slight that only a single curve is shown. The factors $\frac{\sqrt{\eta_{t,s}}}{u/V_t}$ and u/V_t are single-valued functions of each other.

Compressor characteristics.—In compressor practice it is convenient to define the slip factor K_c as

$$K_c=\frac{550\,P_c}{M_aU^2} \tag{7}$$

The conventional presentation of performance curves for a typical centrifugal-flow compressor is given in figure 13 and for an axial-flow compressor in figure 14. The compressor pressure ratio p_2/p_1, adiabatic efficiency η_c, and slip factor K_c are plotted against mass-flow factor $M_a\sqrt{\theta_1}/\delta_1$ for various values of tip-speed factor $U/\sqrt{\theta_1}$.

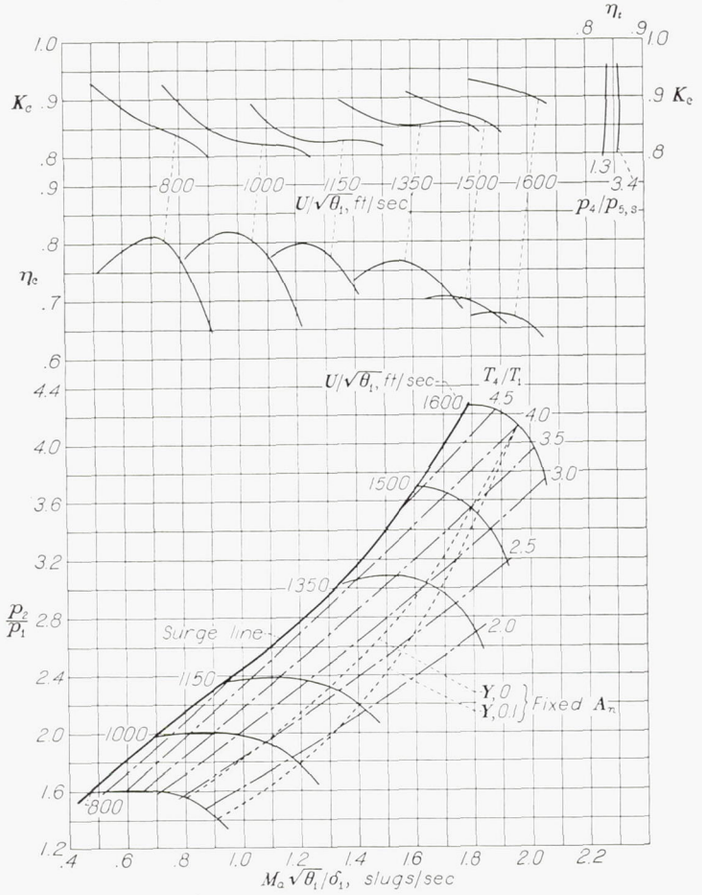


FIGURE 13.—Characteristics of centrifugal-flow compressor.

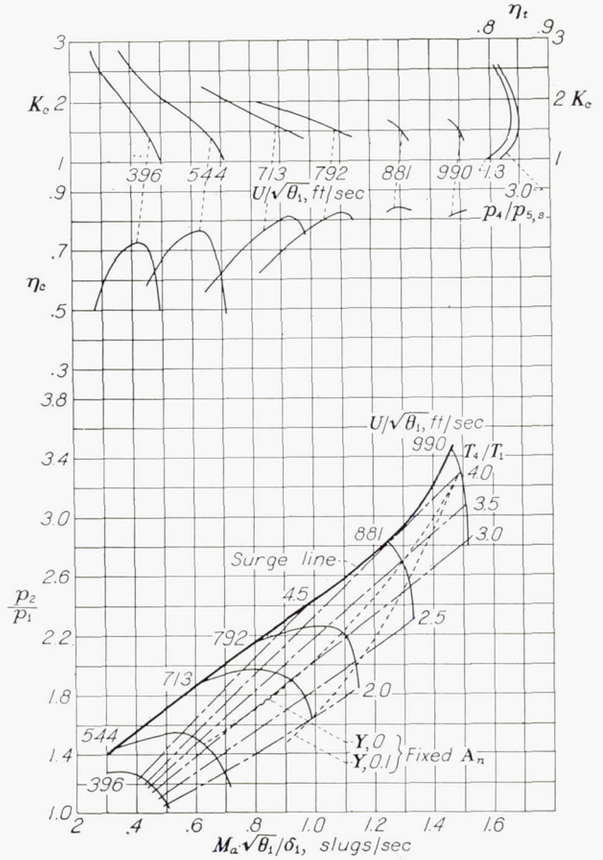


FIGURE 14.—Characteristics of axial-flow compressor.

As the tip speed of the centrifugal-flow compressor increases (fig. 13), both the pressure ratio and mass flow can be increased, however, the compressor efficiency decreases. At a given tip speed, a reduction in mass flow by throttling the compressor outlet results in an increase in pressure ratio and efficiency to peak values. Stalling of the compressor accompanied by surging of the flow occurs at excessive throttling to the positions indicated by the surge line.

The characteristic curves for the axial-flow compressor (fig. 14) are similar in trend to those for the centrifugal-flow compressor with the exceptions that high efficiencies can be obtained at the high tip speeds; operation at a given high tip speed is limited to a much narrower range of mass flow; at a given tip speed, pressure ratio and efficiency decrease more rapidly from the optimum value with change in mass flow; and the value of the slip factor K_c varies appreciably from unity.

The axial-flow compressor shows less loss in efficiency than the centrifugal-flow compressor with increase in pressure ratio in the range of operation shown. The axial-flow compressor has the advantage over the single-stage centrifugal-flow compressor in that it can be designed to maintain high over-all efficiency at any desired pressure ratio by providing a sufficient number of high-efficiency stages. For the centrifugal-flow compressor, an increase in pressure ratio is obtained by an increase in tip speed and hence velocities at the impeller exit, which are in the transonic and supersonic ranges, are eventually involved. The problem arises of converting efficiently these high velocities into pressure in the diffuser section of the compressor.

Matching turbine and compressor.—A compressor and a turbine selected for the engine have to be so matched that the mass-flow factor of the turbine $M_g\sqrt{\theta_4}/\delta_4$ is consistent with that of the compressor $M_a\sqrt{\theta_1}/\delta_1$ when the compressor is operating at its design point and the engine is operating at design temperatures, flight speed, and altitude. The mass-flow factor of the turbine being a function of turbine-nozzle area necessitates this area to be adjusted to give the desired turbine mass-flow factor.

The turbine, whose characteristics are presented in figure 12, is already matched with both the centrifugal-flow and axial-flow compressors for a design-point temperature ratio T_4/T_1 of 4.0. The sizes of the compressors were specially chosen so that the same turbine could be matched with both compressors. The design point of each compressor was chosen at the maximum tip-speed factor $U/\sqrt{\theta_1}$ and at a pressure ratio permitting operation sufficiently far from the surge line to insure stable operation over a wide range of conditions off the design point. For the centrifugal-flow compressor, the value of the design pressure ratio is 4.1, and for the axial-flow compressor it is 3.3.

The lines of constant temperature ratio T_4/T_1 for a matched compressor and turbine set are included on the plots of figures 13 and 14. These lines are obtained as follows: When the difference between M_a and M_g is neglected,

$$\frac{M_a\sqrt{T_1}}{p_1}=\frac{p_4}{p_1}\sqrt{\frac{T_1}{T_4}}\frac{M_g\sqrt{T_4}}{p_4}$$

If r represents the ratio of the drop in combustion-chamber total pressure to the compressor-outlet total pressure, then

$$\Delta p_2=p_2-p_4=rp_2$$

or

$$p_4=(1-r)p_2$$

Hence

$$\frac{M_a\sqrt{T_1}}{p_1}=(1-r)\frac{p_2}{p_1}\sqrt{\frac{T_1}{T_4}}\frac{M_g\sqrt{T_4}}{p_4}$$

or

$$\frac{M_a\sqrt{\theta_1}}{\delta_1}=(1-r)\frac{p_2}{p_1}\sqrt{\frac{T_1}{T_4}}\frac{M_g\sqrt{\theta_4}}{\delta_4} \tag{8}$$

At rotor speeds of the turbojet engine where choking of the flow at the turbine nozzle occurs, the value of $M_g\sqrt{\theta_4}/\delta_4$ becomes constant (for example, in the region of pressure ratios $p_4/p_{5,s}$ above 2.5 for the turbine as shown in fig. 12 (a)). When this constant value of $M_g\sqrt{\theta_4}/\delta_4$ is substituted into equation (8) and a value is assumed for r, it is possible to compute the value T_4/T_1 for desired design values of $M_a\sqrt{\theta_1}/\delta_1$ and p_2/p_1. In the nonchoking zone, the value of $M_g\sqrt{\theta_4}/\delta_4$ is not so easily determined and the more general method described in appendix C is used.

Engine with centrifugal-flow compressor.—In a turbojet engine, the compressor power is equal to the turbine power; hence from equations (6) and (7)

$$K_cU^2=\frac{1}{2}V_t^2\eta_{t,s} \tag{9}$$

(The difference between M_a and M_g has been neglected.) The factor B, which is the ratio of the compressor tip speed U to the turbine-blade speed u, is a constant for any given turbojet engine; so equation (9) becomes

$$K_cB^2=\frac{1}{2}\left(\frac{V_t}{u}\right)^2\eta_{t,s} \tag{10}$$

Any value of K_c thus determines the value of $\eta_{t,s}\left(\frac{V_t}{u}\right)^2$ and hence, from figure 12 (b), determines the values of u/V_t and also determines the values of η_t and $\eta_{t,s}$ when the effect of pressure ratio across the turbine is neglected. A value of B equal to 1.275 was chosen for the engine with a centrifugal-flow compressor. For a compressor for which K_c is nearly constant, the turbine operates at nearly constant blade-to-jet speed ratio and hence nearly constant turbine efficiency over the entire operating range of the engine. For example, over the operating range of the centrifugal-flow compressor under discussion, the value of the slip factor K_c varies between 0.80 and 0.95. The corresponding turbine total efficiencies obtained from equation (10) and figure 12 (b) are shown plotted in figure 13 for two values of $p_4/p_{5,s}$. The value of η_t is substantially constant over the entire range of operation, as shown in figure 13.

At any given rotative speed and compressor-inlet temperature T_1, increasing the combustion-chamber-outlet temperature T_4 is equivalent to throttling the compressor. This increase in T_4 causes an increase in compressor pressure ratio and adiabatic efficiency until peak values are reached. Excessive combustion-chamber-outlet temperature carries operation past peak conditions to surging.

Operation at any point shown in figure 13 at given flight conditions requires a specific exhaust-nozzle area. Thus every point in figure 13 is a possible operating point provided the turbojet engine is equipped with a variable-area exhaust nozzle.

When the engine is provided with a fixed-area exhaust nozzle, then, for any given flight Mach number, operation at any one tip-speed factor $U/\sqrt{\theta_1}$ is limited to one value of p_2/p_1. For the engine equipped with the components shown in figures 12 and 13, an exhaust-nozzle area of 1.42 square feet is required for operation at the design conditions (p_2/p_1, 4.1; $U/\sqrt{\theta_1}$, 1600 ft/sec; T_4/T_1, 4.0; and Y, 0.1). Figure 13 shows the lines of operation of the engine equipped with a fixed-area exhaust nozzle for values of Y of 0 and 0.1. (The method used to determine these lines is described in appendix D.) In the region of high rotative speeds, the jet velocity becomes supersonic so that the exhaust nozzle is choked and the fixed-area lines for the values of Y merge into a single curve. For a fixed-area exhaust nozzle at any given value of Y and compressor-inlet temperature T_1, any change in the combustion-chamber-outlet temperature T_4 is accompanied by variations in $U/\sqrt{\theta_1}$ and p_2/p_1. In the practical range of operation, an increase in T_4 can only be obtained by increasing tip speed and compressor pressure ratio.

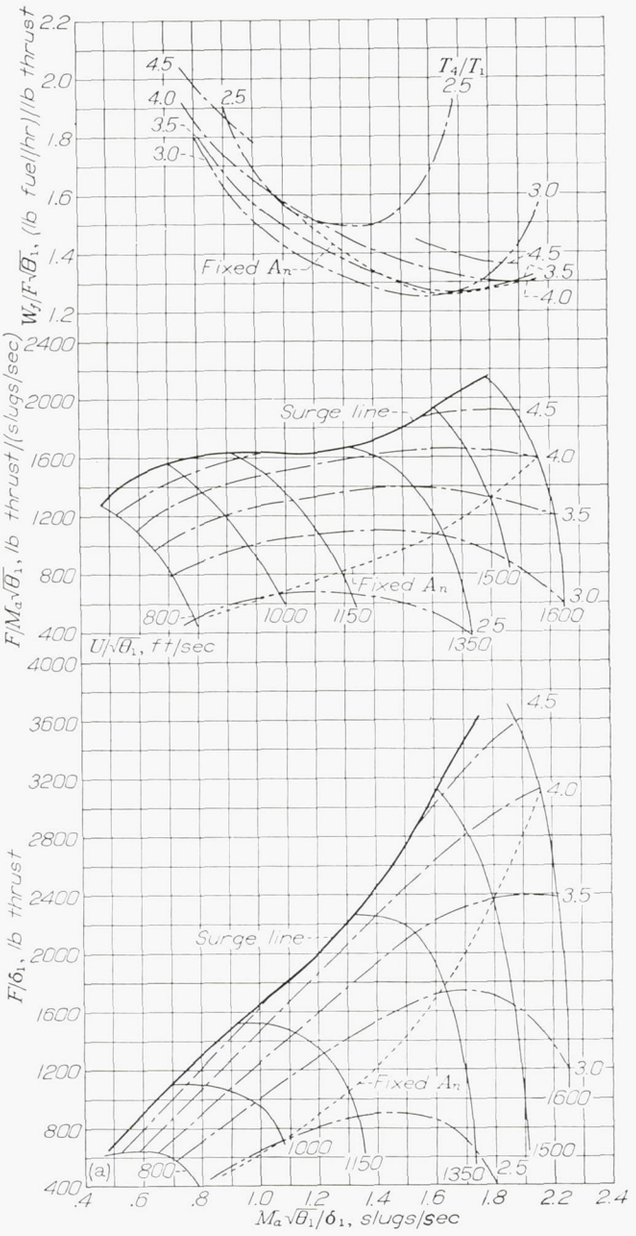
The thrust factor F/δ_1, the thrust-per-unit-mass-rate-of-airflow factor $F/M_a\sqrt{\theta_1}$, and the thrust-specific-fuel-consumption factor $W_f/F\sqrt{\theta_1}$ of the turbojet engine plotted against mass-flow factor $M_a\sqrt{\theta_1}/\delta_1$ in figure 15 correspond to the conditions shown in figure 13 for values of Y of 0 and 0.1 (that is, flight Mach numbers of 0 and 0.707, respectively). The values of F/δ_1 and $F/M_a\sqrt{\theta_1}$ increase appreciably with increase in T_4/T_1.

At the high tip speeds, $F/M_a\sqrt{\theta_1}$ for constant T_4/T_1 decreases with increase in $U/\sqrt{\theta_1}$. This effect is a consequence of the reduction in compressor efficiency that offsets the effect of increased pressure ratio when $U/\sqrt{\theta_1}$ is increased. This effect is more pronounced the lower the value of T_4/T_1. The thrust factor, which is the product of $F/M_a\sqrt{\theta_1}$ and $M_a\sqrt{\theta_1}/\delta_1$, is largely influenced by the increase in mass-flow factor that accompanies the increase in $U/\sqrt{\theta_1}$. At the higher values of T_4/T_1, the thrust factor continues to increase with increasing $U/\sqrt{\theta_1}$; at intermediate values of T_4/T_1, the thrust factor peaks at the higher $U/\sqrt{\theta_1}$, whereas at the lower values of T_4/T_1, the thrust factor is decreasing at high values of $U/\sqrt{\theta_1}$. Every point on figure 15 is a possible operating point if the engine is provided with a variable-area exhaust nozzle. A line of fixed-area-exhaust-nozzle operation is also shown in figure 15.

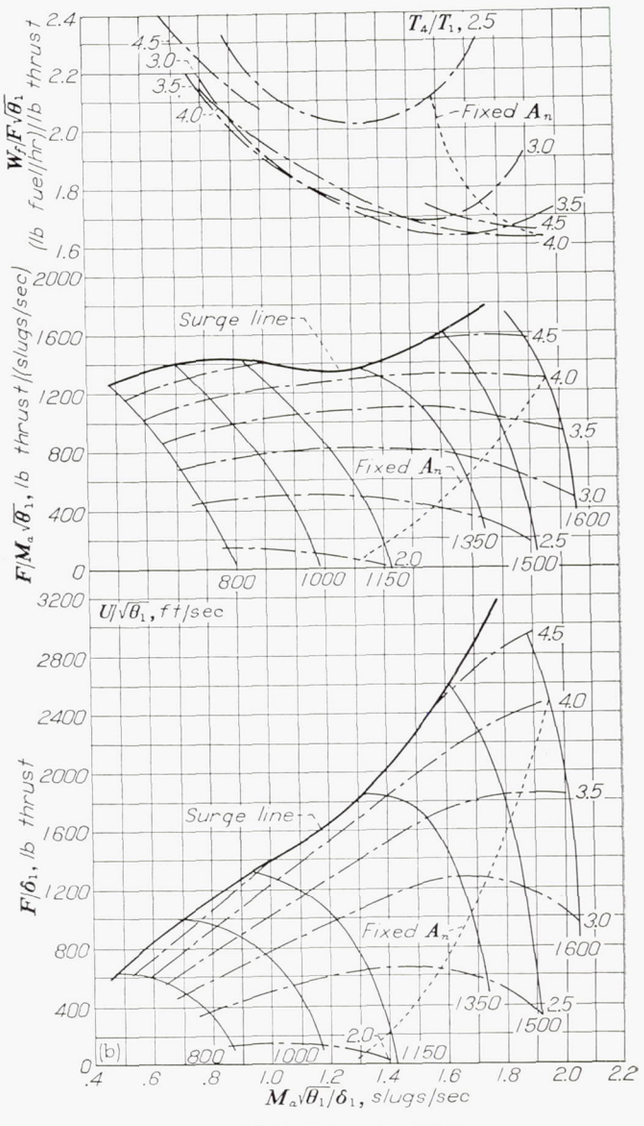
For an engine with a fixed-area exhaust nozzle, the specific fuel consumption over the entire operating range of the engine is shown by the dotted lines on the specific-fuel-consumption plot in figure 15. The point of minimum $W_f/F\sqrt{\theta_1}$, corresponding to any value of $U/\sqrt{\theta_1}$, T_4/T_1, or F/δ_1, generally does not fall on a fixed-area line. The $W_f/F\sqrt{\theta_1}$ curves illustrate this statement for values of T_4/T_1. Further verifying this statement for the other quantities mentioned requires locating lines of constant $U/\sqrt{\theta_1}$ or F/δ_1 on the specific-fuel-consumption curves. (These lines were omitted from the plot for clarity.) In order to obtain these points of minimum specific fuel consumption, a variable-area exhaust nozzle is required.

A variable-area exhaust nozzle also permits obtaining maximum F/δ_1 when values of T_4/T_1 greater than 4.0 are possible and the maximum $U/\sqrt{\theta_1}$ is limited.

In many cases for a given $U/\sqrt{\theta_1}$, minimum $W_f/F\sqrt{\theta_1}$ occurs at an intermediate value of T_4/T_1 even though η_c and p_2/p_1 are less at this intermediate T_4/T_1 than at a higher T_4/T_1. This occurrence becomes evident if lines of constant



(a) Y, 0 (flight Mach number, 0).



(b) Y, 0.1 (flight Mach number, 0.707).

FIGURE 15.—Performance of turbojet engine with centrifugal-flow compressor. (η_b, 0.96; C_v, 0.97; h, 18,900 Btu/lb)

$U/\sqrt{\theta_1}$ are plotted on the $W_f/F\sqrt{\theta_1}$ curves of figure 15. The occurrence of minimum specific fuel consumption at an intermediate temperature was anticipated from figures 8 and 9. Decreasing the turbine-nozzle area (which reduces the mass-flow factor) shifts all temperature lines (fig. 13) toward the surge line, and the T_4/T_1 value corresponding to any point on the compressor curves is reduced. This change in turbine-nozzle area enables an optimum $W_f/F\sqrt{\theta_1}$ at any $U/\sqrt{\theta_1}$ to be obtained because operation at the best combination of T_4/T_1, η_c, and p_2/p_1 can be realized.

Changes in turbine-nozzle area can also be used to improve the thrust factor at any desired engine operating conditions.

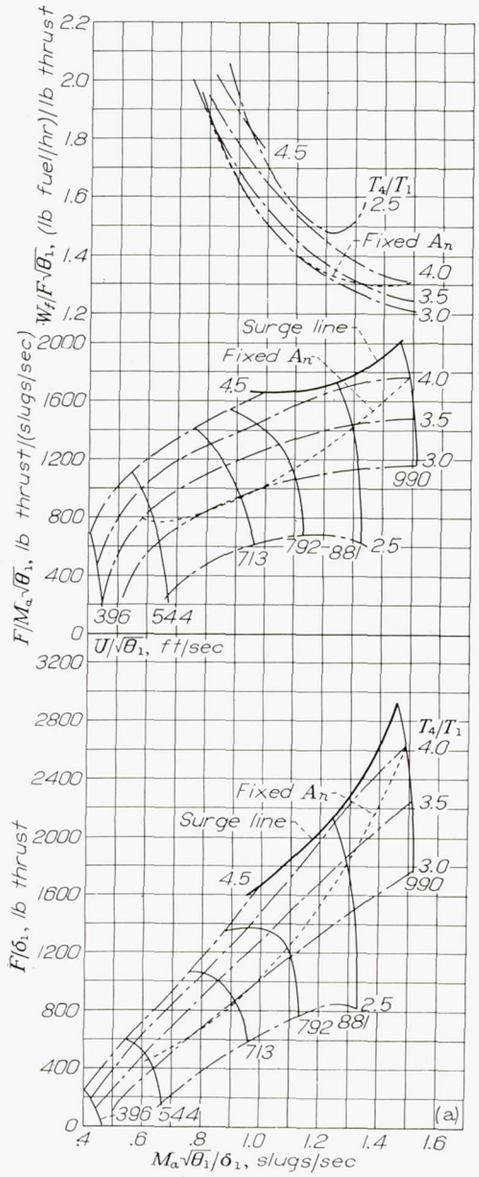
From the foregoing discussion, it is evident that in order to obtain the ultimate in either thrust or specific fuel consumption from a given engine, a variable-area turbine nozzle as well as a variable-area exhaust nozzle are necessary.

Engine with axial-flow compressor.—Figure 14 shows the performance characteristics of the axial-flow compressor used in the second illustrative turbojet engine. At high tip speeds, because operation at any given tip speed is limited to a much narrower range of mass flow for the axial-flow than for the centrifugal-flow compressor, the turbine-flow area must be designed with greater accuracy for the axial-flow than for the centrifugal-flow compressor to obtain a proper match of turbine and compressor characteristics at the design point.

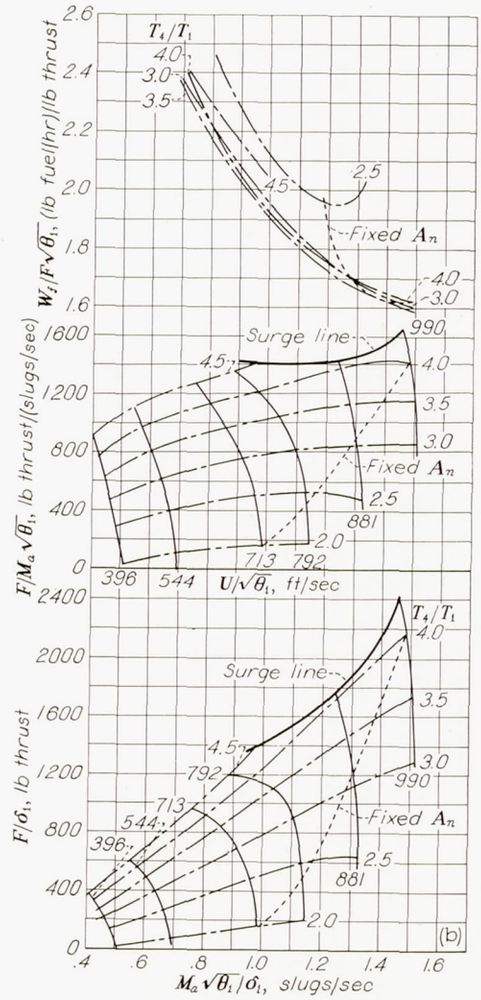
The variation of the factor K_c is much greater for the axial-flow than for the centrifugal-flow compressor. At the high tip speeds, however, the variation in K_c for the axial-flow compressor is sufficiently limited in the practical operating range to provide nearly constant turbine efficiency. The turbine total efficiency curves in figure 14 were obtained from figure 12 and equation (10) and pertain to a turbojet engine incorporating the turbine and the axial-flow compressor characterized by the data in figures 12 and 14, respectively. A value of B equal to 0.97 was chosen for the engine with an axial-flow compressor.

The lines of constant T_4/T_1 for this engine were computed in the manner described in appendix C from the data of figures 12 and 14. The lines for an illustrative fixed-area exhaust nozzle A_n of 1.03 square feet are also shown.

The values of F/δ_1, $F/M_a\sqrt{\theta_1}$, and $W_f/F\sqrt{\theta_1}$ that are shown



(a) Y, 0 (flight Mach number, 0).



(b) Y, 0.1 (flight Mach number, 0.707).

FIGURE 16.—Performance of turbojet engine with axial-flow compressor. (η_b, 0.96; C_p, 0.97; h, 18,900 Btu/lb)

in figure 16 for the turbojet engine correspond to the data of figure 14. The minimum value of the specific-fuel-consumption factor in figure 16 (a) is obtained at a T_4/T_1 value of 3.0 and in figure 16 (b) at a T_4/T_1 value of 3.5. In both cases, minimum specific fuel consumption occurs at the highest tip-speed factor shown. The fact that compressor efficiency does not fall off with increase in tip speed in the range shown contributes to the occurrence of minimum $W_f/F\sqrt{\theta_1}$ at high $U/\sqrt{\theta_1}$.

For a turbojet engine with a fixed-area exhaust nozzle operating at a constant flight Mach number (constant value of Y), figures 13 and 15 or 14 and 16 indicate that the factors F/δ_1, $M_a\sqrt{\theta_1}/\delta_1$, $F/M_a\sqrt{\theta_1}$, T_4/T_1, and $W_f/F\sqrt{\theta_1}$ plotted against $U/\sqrt{\theta_1}$ should result in single curves regardless of the altitude of operation (that is, regardless of ambient pressure and temperature). These single curves occur in practice for all factors except the specific-fuel-consumption factor. In this case, the assumptions of a constant combustion efficiency and a constant specific heat of gases during combustion for a given T_4/T_1 that are required for such correlation are not valid in actual operation.

The performance of the two illustrative turbojet engines presented herein is not indicative of the best performance obtainable with this type of engine because no attempt was made to pick components with optimum characteristics. The purpose of the discussion of these illustrative engines is primarily to provide some insight into the manner in which the performance characteristics of the components influenced the performance of the engine, and some understanding of the basic characteristics and limitations of the turbojet engine.

CONCLUSIONS

For a series of turbojet engines in which the appropriate compressor and turbine are used for given operating conditions, the following conclusions may be drawn:

1. An increase in combustion-chamber-outlet temperature causes an increase in thrust. An optimum temperature exists, however, at which minimum specific fuel consumption is obtained. This temperature for minimum specific fuel consumption is at some conditions less than the temperature limit imposed by strength-temperature characteristics of the materials of current turbojet engines.

2. Maximum thrust per unit mass rate of air flow occurs at a lower compressor pressure ratio than minimum specific fuel consumption.

For a turbojet engine with a given set of matched components, the following conclusions may be drawn:

1. The turbine efficiency remains substantially at the design value even when the engine operating conditions vary appreciably from their design values.

2. At a given flight speed and altitude, a fixed-area exhaust nozzle limits engine operation to a fixed relation between rotative speed and combustion-chamber-outlet temperature.

3. The use of a variable-area exhaust nozzle permits engine operation over a wide range of engine rotative speeds for each combustion-chamber-outlet temperature. The use of this type nozzle, as contrasted with the fixed-area nozzle, thus permits independent adjustment of the engine rotative speed and the combustion-chamber-outlet temperature to obtain lower specific fuel consumption over a range of thrust values.

AIRCRAFT ENGINE RESEARCH LABORATORY,
NATIONAL ADVISORY COMMITTEE FOR AERONAUTICS,
CLEVELAND, OHIO, *June 1, 1946.*

APPENDIX A

EQUATIONS FOR PERFORMANCE CHARTS

In addition to those symbols previously defined, the following symbols are used in these equations:

$\bar{c}_p$ average specific heat at constant pressure of gases during combustion process, Btu/(slug)(°F)
This term, when used with temperature change during combustion, is used to determine fuel consumption.

R_a gas constant of air, 1716 ft-lb/(slug)(°F)

R_g gas constant of exhaust gas, ft-lb/(slug)(°F)

X' factor defined as equal to $\left[\frac{p_2/p_1}{(p_2/p_1)_{ref}}\right]^{\frac{\gamma_a-1}{\gamma_a}}$ or $(X)^{\frac{\gamma_a-1}{\gamma_a}}$

W_{th} ideal work for adiabatic process, ft-lb/slug

(The equation numbers correspond to those in the derivation given in appendix B.)

Figure 2:

$$Y=\frac{V_o^2}{2Jc_{p,a}T_0}=\frac{1}{2Jc_{p,a}519}\left(V_o\sqrt{\frac{519}{T_0}}\right)^2 \tag{B14}$$

$$\frac{p_1+\Delta p_d}{p_0}=\left[1+\frac{1}{2Jc_{p,a}519}\left(V_o\sqrt{\frac{519}{T_0}}\right)^2\right]^{\frac{\gamma_a}{\gamma_a-1}} \tag{B70}$$

$$\text{Flight Mach number}=\sqrt{\frac{1}{(\gamma_a-1)Jc_{p,a}519}}\left(V_o\sqrt{\frac{519}{T_0}}\right) \tag{B72}$$

Figure 3 (a):

$$a=\frac{\Delta p_d}{p_1}\left(\frac{\gamma_a-1}{\gamma_a}\right)\left(\frac{1}{Y+\eta_c Z}\right) \tag{B45}$$

Figure 3 (b):

$$b=\frac{\Delta p_2}{p_2}\left(\frac{\gamma_a-1}{\gamma_a}\right)\left(\frac{1}{Y+\eta_c Z}\right) \tag{B46}$$

Figure 3 (c):

$$c=\frac{\frac{W_{th}}{R_gT_4}}{\left(\frac{\gamma_a}{\gamma_a-1}\right)\left[1-\left(\frac{p_0}{p_2}\right)^{\frac{\gamma_a-1}{\gamma_a}}\right]}\frac{R_g}{R_a}-1 \tag{B52}$$

where values of W_{th}/R_gT_4 are obtained from reference 8.

Figure 4:

$$\frac{p_2}{p_1}=\left(1+\frac{\eta_c Z}{1+Y}\right)^{\frac{\gamma_a}{\gamma_a-1}} \tag{B20}$$

$$\left(\frac{p_2}{p_1}\right)_{ref}=\left[\eta_c\eta_t\epsilon\frac{T_4}{T_0}\left(\frac{1}{1+Y}\right)^2\right]^{\frac{\gamma_a}{2(\gamma_a-1)}} \tag{B66}$$

Figure 5 (a):

$$V_j\sqrt{\frac{\eta_c\eta_t}{C_v^2}\frac{519}{T_0}}=$$

$$\sqrt{2Jc_{p,a}519\left[\eta_c\eta_t\epsilon\frac{T_4}{T_0}-\left(X'+\frac{1}{X'}\right)\sqrt{\eta_c\eta_t\epsilon\frac{T_4}{T_0}+1}\right]+\frac{519}{T_0}V_o^2} \tag{B43}$$

where X' is equal to $(X)^{\frac{\gamma_a-1}{\gamma_a}}$

Figure 5 (b):

$$\frac{\Delta V_j}{V_j}=\frac{\frac{1}{2}\left[1-\left(\frac{C_vV_5}{V_j}\right)^2\right]\left(\frac{1}{\eta_t}-1\right)}{\frac{T_4}{T_0Z}\frac{c_{p,g}}{c_{p,a}}-1} \tag{B64}$$

Figure 6:

$$H_2=c_{p,a}T_0(1+Y+Z) \tag{B36}$$

The T_2 corresponding to the enthalpy H_2 is obtained from reference 6.

Figure 7:

$$\eta_b f=\frac{\bar{c}_p(T_4-T_2)}{32.2h} \tag{B33}$$

where $\bar{c}_p$ is determined from reference 7.

APPENDIX B

DERIVATION OF PERFORMANCE EQUATIONS AND MISCELLANEOUS EXPRESSIONS

From the momentum equation, the net jet thrust when the effect of mass of added fuel is neglected is

$$F=M_a(V_j-V_o) \tag{B1a}$$

and when the mass of added fuel is included

$$F=M_a(V_j-V_o)+fM_aV_j \tag{B1b}$$

The thrust horsepower developed by the jet is

$$thp=\frac{FV_o}{550} \tag{B2}$$

By definition, the turbine total efficiency is

$$\eta_t=\frac{550\ P_t}{(1+f)M_aJc_{p,g}T_4\left[1-\left(\frac{p_{5,8}}{p_4}\right)^{\frac{\gamma_g-1}{\gamma_g}}\right]-(1+f)\ \frac{M_aV_5^2}{2}} \tag{B3}$$

The jet velocity (when the effect of reheat due to turbine losses, which occurs in the further expansion of the gases from turbine-outlet static pressure to ambient-air pressure, is neglected) is given by

$$V_j=C_v\sqrt{2Jc_{p,g}T_4\left[1-\left(\frac{p_0}{p_4}\right)^{\frac{\gamma_g-1}{\gamma_g}}\right]-\frac{550\ P_t}{\frac{1}{2}\ M_a\eta_t(1+f)}} \tag{B4}$$

For simplification, the effect of added fuel is neglected by dropping the term f in equation (B4). The effect of the presence of fuel on jet velocity V_j can be taken into account in the subsequent equations and in the charts for V_j by using, for the value of η_t, the product of the turbine efficiency η_t and $(1+f)$ inasmuch as the quantities η_t and f appear only as the product $\eta_t(1+f)$ in equation (B4). Now

$$\left[1-\left(\frac{p_0}{p_4}\right)^{\frac{\gamma_g-1}{\gamma_g}}\right]=1-\left(\frac{p_0}{p_2}\right)^{\frac{\gamma_g-1}{\gamma_g}}\left(1-\frac{\Delta p_2}{p_2}\right)^{-\frac{\gamma_g-1}{\gamma_g}} \tag{B5}$$

and when the last term is expanded into a series

$$\left(1-\frac{\Delta p_2}{p_2}\right)^{-\frac{\gamma_g-1}{\gamma_g}}=1+\frac{\gamma_g-1}{\gamma_g}\ \frac{\Delta p_2}{p_2} \tag{B6}$$

for small $\frac{\Delta p_2}{p_2}$. Because only enough turbine power is removed to drive the compressor

$$P_t=P_c \tag{B7}$$

When equations (B5), (B6), and (B7) are substituted into equation (B4)

$$V_j=C_v\sqrt{2Jc_{p,g}T_4\left[1-\left(\frac{p_0}{p_2}\right)^{\frac{\gamma_g-1}{\gamma_g}}\right]-2Jc_{p,g}T_4\left(\frac{p_0}{p_2}\right)^{\frac{\gamma_g-1}{\gamma_g}}\left(\frac{\gamma_g-1}{\gamma_g}\right)\frac{\Delta p_2}{p_2}-\frac{550P_c}{\frac{1}{2}M_a\eta_t}} \tag{B8}$$

Let

$$K=\frac{c_{p,g}\left[1-\left(\frac{p_0}{p_2}\right)^{\frac{\gamma_g-1}{\gamma_g}}\right]}{c_{p,a}\left[1-\left(\frac{p_0}{p_2}\right)^{\frac{\gamma_a-1}{\gamma_a}}\right]} \tag{B9}$$

and

$$K'=\frac{\left(\frac{p_0}{p_2}\right)^{\frac{\gamma_g-1}{\gamma_g}}\left(\frac{\gamma_g-1}{\gamma_g}\right)c_{p,g}}{\left(\frac{p_0}{p_2}\right)^{\frac{\gamma_a-1}{\gamma_a}}\left(\frac{\gamma_a-1}{\gamma_a}\right)c_{p,a}} \tag{B10}$$

When equations (B9) and (B10) are used in equation (B8)

$$V_j=C_v\sqrt{2Jc_{p,a}T_4\left[1-\left(\frac{p_0}{p_2}\right)^{\frac{\gamma_a-1}{\gamma_a}}\right]K-2Jc_{p,a}T_4\left(\frac{p_0}{p_2}\right)^{\frac{\gamma_a-1}{\gamma_a}}\left(\frac{\gamma_a-1}{\gamma_a}\right)\frac{\Delta p_2}{p_2}K'-\frac{550\ P_c}{\frac{1}{2}\ M_a\eta_t}} \tag{B11}$$

The total temperature at the compressor inlet (which is equal to the total temperature of the inlet air) is

$$T_1=T_0+\frac{V_o^2}{2Jc_{p,a}} \tag{B12}$$

The ideal stagnation pressure $p_{1,i}$ corresponding to this total temperature is

$$p_{1,i}=p_0\left(1+\frac{V_o^2}{2Jc_{p,a}T_0}\right)^{\frac{\gamma_a}{\gamma_a-1}} \tag{B13}$$

Define

$$Y=\frac{V_o^2}{2Jc_{p,a}T_0} \tag{B14}$$

so that

$$T_1=T_0(1+Y) \tag{B15}$$

and

$$\frac{p_{1,i}}{p_0}=(1+Y)^{\frac{\gamma_a}{\gamma_a-1}} \tag{B16}$$

The compressor-shaft horsepower expressed as a function of compressor-inlet temperature and pressure ratio is

$$P_c=\frac{M_a Jc_{p,a}T_1}{550\eta_c}\left[\left(\frac{p_2}{p_1}\right)^{\frac{\gamma_a-1}{\gamma_a}}-1\right] \tag{B17}$$

where the specific heats of air during the compression process are assumed constant. Because of this assumption, the value of the compressor-shaft horsepower calculated from equation (B17) for a given pressure ratio, inlet temperature, and efficiency is slightly greater than the actual compressor power. The deviation increases with increasing pressure ratio and inlet temperature. For values of T_1 up to 550° R and p_2/p_1 up to 40, the maximum error in compressor work is about 1 percent.

Define

$$Z=\frac{550P_c}{M_a Jc_{p,a}T_0} \tag{B18}$$

so that substituting equations (B15) and (B17) into equation (B18) results in

$$\eta_c Z=(1+Y)\left[\left(\frac{p_2}{p_1}\right)^{\frac{\gamma_a-1}{\gamma_a}}-1\right] \tag{B19}$$

or

$$\frac{p_2}{p_1}=\left(1+\frac{\eta_c Z}{1+Y}\right)^{\frac{\gamma_a}{\gamma_a-1}}=\left(\frac{1+Y+\eta_c Z}{1+Y}\right)^{\frac{\gamma_a}{\gamma_a-1}} \tag{B20}$$

Now

$$p_1=p_{1,i}-\Delta p_d \tag{B21}$$

so that

$$\frac{p_1}{p_0}=\frac{p_{1,i}}{p_0}-\frac{\Delta p_d}{p_1}\frac{p_1}{p_0} \tag{B22}$$

from which

$$\frac{p_1}{p_0}=\frac{\frac{p_{1,i}}{p_0}}{1+\frac{\Delta p_d}{p_1}} \tag{B23}$$

When equation (B16) is used in equation (B23)

$$\frac{p_1}{p_0}=\frac{(1+Y)^{\frac{\gamma_a}{\gamma_a-1}}}{1+\frac{\Delta p_d}{p_1}} \tag{B24}$$

Equations (B20) and (B24) are combined so that

$$\frac{p_0}{p_2}=\frac{1+\frac{\Delta p_d}{p_1}}{(1+Y+\eta_c Z)^{\frac{\gamma_a}{\gamma_a-1}}} \tag{B25}$$

Therefore

$$1-\left(\frac{p_0}{p_2}\right)^{\frac{\gamma_a-1}{\gamma_a}}=1-\frac{\left(1+\frac{\Delta p_d}{p_1}\right)^{\frac{\gamma_a-1}{\gamma_a}}}{1+Y+\eta_c Z} \tag{B26}$$

Expand

$$\left(1+\frac{\Delta p_d}{p_1}\right)^{\frac{\gamma_a-1}{\gamma_a}}=1+\frac{\gamma_a-1}{\gamma_a}\frac{\Delta p_d}{p_1} \tag{B27}$$

which is accurate for small values of $\Delta p_d/p_1$.

When equations (B18), (B25), (B26), and (B27) are used in equation (B11)

$$\frac{V_j}{C_v}=\sqrt{2Jc_{p,a}T_0}\sqrt{K\frac{T_4}{T_0}\left[\frac{Y+\eta_c Z}{1+Y+\eta_c Z}-\left(\frac{\gamma_a-1}{\gamma_a}\right)\left(\frac{\Delta p_d}{p_1}\right)\frac{1}{1+Y+\eta_c Z}\right]-K'\frac{T_4}{T_0}\left(\frac{\gamma_a-1}{\gamma_a}\right)\frac{\Delta p_2}{p_2}\left[\frac{1}{1+Y+\eta_c Z}+\frac{\left(\frac{\gamma_a-1}{\gamma_a}\right)\left(\frac{\Delta p_d}{p_1}\right)}{1+Y+\eta_c Z}\right]-\frac{Z}{\eta_t}} \tag{B28}$$

The term involving the product of the pressure-drop ratios $\frac{\Delta p_d}{p_1}\frac{\Delta p_2}{p_2}$ can be neglected, so that equation (B28) becomes

$$\frac{V_j}{C_v}=\sqrt{2Jc_{p,a}T_0}\sqrt{K\frac{T_4}{T_0}\frac{Y+\eta_c Z}{1+Y+\eta_c Z}-K\frac{T_4}{T_0}\left(\frac{\gamma_a-1}{\gamma_a}\right)\left(\frac{\Delta p_d}{p_1}\right)\frac{1}{1+Y+\eta_c Z}-K'\frac{T_4}{T_0}\left(\frac{\gamma_a-1}{\gamma_a}\right)\left(\frac{\Delta p_2}{p_2}\right)\frac{1}{1+Y+\eta_c Z}-\frac{Z}{\eta_t}} \tag{B29}$$

The factor ϵ is defined by the equation

$$\frac{V_j}{C_v}=\sqrt{2Jc_{p,a}T_0}\sqrt{\frac{T_4}{T_0}\frac{Y+\eta_cZ}{1+Y+\eta_cZ}\epsilon-\frac{Z}{\eta_t}} \tag{B30}$$

from which

$$\epsilon=K-K\left(\frac{\gamma_a-1}{\gamma_a}\right)\left(\frac{\Delta p_a}{p_1}\right)\left(\frac{1}{Y+\eta_cZ}\right)-$$
$$K'\left(\frac{\gamma_a-1}{\gamma_a}\right)\left(\frac{\Delta p_2}{p_2}\right)\left(\frac{1}{Y+\eta_cZ}\right) \tag{B31}$$

When equations (B30) and (B14) are substituted into equation (B1a)

$$\frac{F}{M_a}=\sqrt{2Jc_{p,a}T_0}\left(C_v\sqrt{\frac{T_4}{T_0}\epsilon\frac{Y+\eta_cZ}{1+Y+\eta_cZ}}-\frac{\eta_cZ}{\eta_c\eta_t}-\sqrt{Y}\right) \tag{B32}$$

FUEL CONSUMPTION

The expression for the fuel-air-ratio factor to obtain a rise in total temperature in the combustion chamber from T_2 to T_4 is

$$\eta_b f=\frac{\overline{c}_p(T_4-T_2)}{32.2h} \tag{B33}$$

where values of $\overline{c}_p$ are determined from reference 7.

From the conservation of energy

$$H_2=H_0+\frac{V_o^2}{2J}+550\frac{P_c}{M_aJ} \tag{B34}$$

where H_2 is the enthalpy of the air corresponding to the compressor-outlet total temperature T_2 in Btu per slug. (Zero enthalpy is arbitrarily fixed at absolute zero temperature.) The symbol H_0 is the enthalpy of air corresponding to the ambient-air temperature T_0 in Btu per slug and is given by

$$H_0=c_{p,a}T_0 \tag{B35}$$

If equations (B35), (B14), and (B18) are used in equation (B34)

$$H_2=c_{p,a}T_0(1+Y+Z) \tag{B36}$$

Now T_2 is a function only of H_2

$$T_2=\phi(H_2)=\phi(c_{p,a}T_0[1+Y+Z]) \tag{B37}$$

and the T_2 corresponding to the enthalpy H_2 is obtained from reference 6.

PRESSURE RATIO FOR OPTIMUM THRUST PER UNIT MASS RATE OF AIR FLOW

For a given V_o, T_0, T_4, η_c, η_t, and C_v, and neglecting the change in ϵ due to a change in η_cZ, the maximum thrust per unit mass rate of air flow with respect to compressor power input (or pressure ratio) is obtained from equation (B32) when

$$\frac{\partial\left(\frac{F}{M_a}\right)}{\partial(\eta_cZ)}=0=\epsilon\frac{T_4}{T_0}\frac{1}{(1+Y+\eta_cZ)^2}-\frac{1}{\eta_c\eta_t} \tag{B38}$$

from which

$$1+Y+(\eta_cZ)_{ref}=\sqrt{\eta_c\eta_t\epsilon\frac{T_4}{T_0}} \tag{B39}$$

(The term $(\eta_cZ)_{ref}$ is used to designate the value of η_cZ for which F/M_a as given by equation (B32) is a maximum.)

Factor X' is defined by the relation

$$X'=\frac{1+Y+\eta_cZ}{1+Y+(\eta_cZ)_{ref}} \tag{B40}$$

hence

$$1+Y+\eta_cZ=X'\sqrt{\eta_c\eta_t\epsilon\frac{T_4}{T_0}} \tag{B41}$$

JET VELOCITY AND THRUST PER UNIT MASS RATE OF AIR FLOW IN TERMS OF FACTOR X'

When equation (B41) is used in equation (B30)

$$\frac{V_j}{C_v}=\sqrt{\frac{2Jc_{p,a}T_0}{\eta_c\eta_t}}\sqrt{\eta_c\eta_t\epsilon\frac{T_4}{T_0}\left(\frac{X'\sqrt{\eta_c\eta_t\epsilon\frac{T_4}{T_0}}-1}{X'\sqrt{\eta_c\eta_t\epsilon\frac{T_4}{T_0}}}\right)-X'\sqrt{\eta_c\eta_t\epsilon\frac{T_4}{T_0}}+1+Y}$$

so that

$$V_j\sqrt{\frac{\eta_c\eta_t}{C_v^2}\frac{519}{T_0}}=\sqrt{2Jc_{p,a}519}\sqrt{\eta_c\eta_t\epsilon\frac{T_4}{T_0}-\left(X'+\frac{1}{X'}\right)\sqrt{\eta_c\eta_t\epsilon\frac{T_4}{T_0}}+1+Y} \tag{B42}$$

which when using equation (B14) can also be written as

$$V_j\sqrt{\frac{\eta_c\eta_t}{C_v^2}\frac{519}{T_0}}=\sqrt{2Jc_{p,a}519\left[\eta_c\eta_t\epsilon\frac{T_4}{T_0}-\left(X'+\frac{1}{X'}\right)\sqrt{\eta_c\eta_t\epsilon\frac{T_4}{T_0}}+1\right]+\frac{519}{T_0}V_o^2} \tag{B43}$$

In terms of X', equation (B32) becomes

$$\frac{F}{M_a}\sqrt{\frac{519}{T_0}}=\sqrt{2Jc_{p,a}519}\left[\sqrt{\frac{C_v^2}{\eta_c\eta_t}}\sqrt{\eta_c\eta_t\epsilon\frac{T_4}{T_0}}-\left(X'+\frac{1}{X'}\right)\sqrt{\eta_c\eta_t\epsilon\frac{T_4}{T_0}}+1+Y-\sqrt{Y}\right] \tag{B44}$$

EVALUATION OF CORRECTION FACTOR ϵ

The factors a and b are

$$a=\frac{\Delta p_d}{p_1}\left(\frac{\gamma_a-1}{\gamma_a}\right)\left(\frac{1}{Y+\eta_c Z}\right) \tag{B45}$$

and

$$b=\frac{\Delta p_2}{p_2}\left(\frac{\gamma_a-1}{\gamma_a}\right)\left(\frac{1}{Y+\eta_c Z}\right) \tag{B46}$$

When equations (B45) and (B46) are substituted into equation (B31)

$$\epsilon=K-Ka-K'b \tag{B47}$$

The terms K and K' are close to unity in value, whereas the values of a and b are small in comparison with unity; therefore, only a very small error is introduced by letting

$$\epsilon=K-a-b \tag{B48}$$

The quantity c is defined as

$$c=K-1 \tag{B49}$$

then

$$\epsilon=1-a-b+c \tag{B50}$$

Now, from equation (B9) and reference 8

$$K=\frac{\frac{W_{th}}{R_g T_4}}{\left(\frac{\gamma_a}{\gamma_a-1}\right)\left[1-\left(\frac{p_0}{p_2}\right)^{\frac{\gamma_a-1}{\gamma_a}}\right]}\frac{R_g}{R_a} \tag{B51}$$

where the values of $W_{th}/R_g T_4$ are obtained from reference 8. These values correspond to the temperature T_4 and pressure ratio p_2/p_0. Therefore,

$$c=\frac{\frac{W_{th}}{R_g T_4}}{\left(\frac{\gamma_a}{\gamma_a-1}\right)\left[1-\left(\frac{p_0}{p_2}\right)^{\frac{\gamma_a-1}{\gamma_a}}\right]}\frac{R_g}{R_a}-1 \tag{B52}$$

CORRECTION FOR REHEAT ACCOMPANYING IRREVERSIBILITY IN TURBINE

The actual jet velocity including reheat in the turbine is given by the equation

$$\frac{V_j^2}{C_v^2}-V_5^2=2Jc_{p,g}T_{5,s}\left[1-\left(\frac{p_0}{p_{5,s}}\right)^{\frac{\gamma_g-1}{\gamma_g}}\right] \tag{B53}$$

The static gas temperature at the turbine outlet is $T_{5,s}$. From equation (B53) the following equation in terms of differentials is obtained:

$$\frac{2V_j}{C_v^2}dV_j=2Jc_{p,g}\left[1-\left(\frac{p_0}{p_{5,s}}\right)^{\frac{\gamma_g-1}{\gamma_g}}\right]dT_{5,s} \tag{B54}$$

When equation (B53) is used in equation (B54),

$$\frac{2V_j}{C_v^2}dV_j=\left(\frac{V_j^2}{C_v^2}-V_5^2\right)\frac{dT_{5,s}}{T_{5,s}} \tag{B55}$$

The independent variable is $T_{5,s}$, therefore

$$\Delta T_{5,s}\equiv dT_{5,s}$$

For small values of $\Delta T_{5,s}$

$$\Delta V_j\approx dV_j \tag{B56}$$

If these expressions for $dT_{5,s}$ and dV_j are used in equation (B55),

$$\frac{\Delta V_j}{V_j}=\frac{1}{2}\left[1-\left(\frac{C_v V_5}{V_j}\right)^2\right]\frac{\Delta T_{5,s}}{T_{5,s}} \tag{B57}$$

The amount of reheat $\Delta T_{5,s}$ is equal to

$$\Delta T_{5,s}=\frac{550P_t}{M_a Jc_{p,g}}\left(\frac{1}{\eta_t}-1\right) \tag{B58}$$

whereas the static gas temperature at the turbine outlet

$$T_{5,s}=T_4-\frac{550P_t}{M_a Jc_{p,g}}-\frac{V_5^2}{2Jc_{p,g}} \tag{B59}$$

In equations (B58) and (B59), the effect of added fuel on gas flow through the turbine is neglected (that is, $M_a=M_g$).

When equations (B7), (B14), and (B18) are used in equations (B58) and (B59),

$$\Delta T_{5,s}=T_0 Z\left(\frac{c_{p,a}}{c_{p,g}}\right)\left(\frac{1}{\eta_t}-1\right) \tag{B60}$$

$$T_{5,s}=T_4-T_0 Z\left(\frac{c_{p,a}}{c_{p,g}}\right)-\frac{V_5^2}{V_o^2}T_0 Y\frac{c_{p,a}}{c_{p,g}} \tag{B61}$$

and when equations (B60) and (B61) are substituted into equation (B57),

$$\frac{\Delta V_j}{V_j}=\frac{\frac{1}{2}\left[1-\left(\frac{C_v V_5}{V_j}\right)^2\right]T_0 Z\frac{c_{p,a}}{c_{p,g}}\left(\frac{1}{\eta_t}-1\right)}{T_4-T_0 Z\frac{c_{p,a}}{c_{p,g}}-\frac{V_5^2}{V_o^2}T_0 Y\frac{c_{p,a}}{c_{p,g}}} \tag{B62}$$

or

$$\frac{\Delta V_j}{V_j}=\frac{\frac{1}{2}\left[1-\left(\frac{C_v V_5}{V_j}\right)^2\right]\left(\frac{1}{\eta_t}-1\right)}{\frac{T_4}{T_0 Z}\frac{c_{p,g}}{c_{p,a}}-1-\frac{V_5^2 Y}{V_o^2 Z}} \tag{B63}$$

The $\frac{V_5^2 Y}{V_o^2 Z}$ term in the denominator is small in comparison with $\frac{T_4}{T_0 Z}\frac{c_{p,g}}{c_{p,a}}-1$ and can be neglected, resulting in

$$\frac{\Delta V_j}{V_j}=\frac{\frac{1}{2}\left[1-\left(\frac{C_v V_5}{V_j}\right)^2\right]\left(\frac{1}{\eta_t}-1\right)}{\frac{T_4}{T_0 Z}\frac{c_{p,g}}{c_{p,a}}-1} \tag{B64}$$

DERIVATION OF MISCELLANEOUS EXPRESSIONS

(a) The reference pressure ratio $(p_2/p_1)_{ref}$ corresponding to any values of Y and of $(\eta_c Z)_{ref}$ from equation (B20) is

$$\left(\frac{p_2}{p_1}\right)_{ref}=\left[\frac{1+Y+(\eta_c Z)_{ref}}{1+Y}\right]^{\frac{\gamma_a}{\gamma_a-1}} \tag{B65}$$

or substituting equation (B39) in equation (B65) gives

$$\left(\frac{p_2}{p_1}\right)_{ref}=\left[\eta_c\eta_t\epsilon\frac{T_4}{T_0}\left(\frac{1}{1+Y}\right)^2\right]^{\frac{\gamma_a}{2(\gamma_a-1)}} \tag{B66}$$

(b) From equations (B40), (B20), and (B65) it is seen that

$$X'=\left[\frac{p_2/p_1}{(p_2/p_1)_{ref}}\right]^{\frac{\gamma_a-1}{\gamma_a}} \tag{B67}$$

or defining the factor X as

$$X=(X')^{\frac{\gamma_a}{\gamma_a-1}} \tag{B68}$$

then

$$X=\frac{p_2/p_1}{(p_2/p_1)_{ref}} \tag{B69}$$

(c) The ideal ram pressure ratio given by equation (B13) can be rewritten as

$$\frac{p_{1,i}}{p_0}=\frac{p_1+\Delta p_d}{p_0}=\left[1+\frac{1}{2Jc_{p,a}519}\left(V_o\sqrt{\frac{519}{T_0}}\right)^2\right]^{\frac{\gamma_a}{\gamma_a-1}} \tag{B70}$$

(d) The flight Mach number is

$$\text{Flight Mach number}=\frac{V_o}{\sqrt{\gamma_aR_aT_0}} \tag{B71}$$

$$=\sqrt{\frac{1}{(\gamma_a-1)Jc_{p,a}519}}\left(V_o\sqrt{\frac{519}{T_0}}\right) \tag{B72}$$

or when equation (B14) is used in equation (B72),

$$\text{Flight Mach number}=\frac{\sqrt{2Jc_{p,a}T_0Y}}{\sqrt{\gamma_aR_aT_0}}=\sqrt{\left(\frac{2}{\gamma_a-1}\right)Y} \tag{B73}$$

APPENDIX C

METHOD FOR DETERMINING CONSTANT T_4/T_1 OPERATING LINES OF MATCHED SET OF TURBOJET COMPONENTS

The procedure for plotting lines of constant T_4/T_1 on compressor-characteristic curves, as in figure 13, for a given turbojet engine is as follows:

Equation (9) may be written

$$K_c \frac{U^2}{\theta_1} = \frac{1}{2} \frac{V_t^2}{\theta_4} \eta_{t,s} \frac{T_4}{T_1} \tag{C1}$$

When T_4/T_1 is eliminated between equations (8) and (C1),

$$\sqrt{K_c} \left(\frac{M_a}{\delta_1} \sqrt{\theta_1} \right) \frac{U}{\sqrt{\theta_1}} = (1-r) \frac{p_2}{p_1} \frac{M_g V_t}{\delta_4} \sqrt{\frac{\eta_{t,s}}{2}} \tag{C2}$$

The method of using equation (C2) to obtain constant T_4/T_1 lines is illustrated for the turbojet engine with a centrifugal-flow compressor.

1. A point on figure 13 is selected at a value of $U/\sqrt{\theta_1}$ and of p_2/p_1 for which the value of T_4/T_1 is desired.

2. The corresponding values of $M_a\sqrt{\theta_1}/\delta_1$, K_c, and an approximate value of η_t are read from figure 13.

3. An approximate value of $\eta_{t,s}$ from figure 12 (b) that corresponds to the approximate value of η_t is used to compute an approximate value of u/V_t from equation (10).

4. For a given value of r, the approximate value of $M_g V_t/\delta_4$ is computed from equation (C2).

5. The value of $V_t/\sqrt{\theta_4}$, corresponding to the values of $M_g V_t/\delta_4$ and u/V_t previously obtained, and the value of $M_g\sqrt{\theta_4}/\delta_4$ are read from figure 12 (a).

6. From equation (8), T_4/T_1 is computed. This value is a first approximation and in most cases is sufficiently accurate.

7. In order to evaluate a second approximation of T_4/T_1, a new value of u/V_t is computed from the identity

$$\frac{u}{V_t} = \frac{U/\sqrt{\theta_1}}{BV_t/\sqrt{\theta_4}} \sqrt{\frac{T_1}{T_4}}$$

8. From figure 12 (b), a new value of $\eta_{t,s}$ is determined from the new value of u/V_t and the value of $p_4/p_{5,s}$ corresponding to the previous value of $V_t/\sqrt{\theta_4}$ as determined in step 5.

9. Steps 4, 5, and 6 are repeated.

In order to illustrate this procedure, the temperature ratio corresponding to a point on the centrifugal-flow-compressor-characteristic curve is evaluated. For the turbojet engine with a centrifugal-flow compressor, a compressor-tip-speed to turbine-blade-speed ratio B of 1.275 is used.

1. The point at $U/\sqrt{\theta_1}$ of 1600 (ft/sec) and p_2/p_1 of 4.0 is selected.

2. Corresponding to this point, $M_a\sqrt{\theta_1}/\delta_1$ is 2.0 (slug/sec), K_c is 0.945, and the approximate η_t is 0.85.

3. The corresponding $\eta_{t,s}$ (from fig. 12 (b)) is 0.80 and the value of u/V_t evaluated from equation (10) is 0.51.

4. For a value of r of 0.05, the value of $M_g V_t/\delta_4$ is 1295 ((slug)(ft)/sec^2), as determined from equation (C2).

5. Corresponding to the values of $M_g V_t/\delta_4$ and u/V_t, values of $V_t/\sqrt{\theta_4}$ of 1295 (ft/sec), $M_g\sqrt{\theta_4}/\delta_4$ of 1.0 (slug/sec), and $p_4/p_{5,s}$ of 2.92 are obtained from figure 12 (a).

6. A value of T_4/T_1 of 3.61 is obtained using equation (8). This is the first approximation.

7. From the identity

$$\frac{u}{V_t} = \frac{U/\sqrt{\theta_1}}{BV_t/\sqrt{\theta_4}} \sqrt{\frac{T_1}{T_4}}$$

a value of u/V_t of 0.51 is obtained.

8. At this value of u/V_t in figure 12 (b), values of η_t of 0.85 and $\eta_{t,s}$ of 0.80 are obtained, which are the same as the values determined in steps 2 and 3; therefore no further approximations are necessary.

APPENDIX D

METHOD FOR DETERMINING FIXED-EXHAUST-NOZZLE-AREA OPERATING LINES OF MATCHED SET OF TURBOJET COMPONENTS

Useful equations for determining the values of several parameters needed in this method are as follows:

$$\frac{V_j}{\sqrt{\theta_5}}=C_v\sqrt{2Jc_{p,g}519\left[1-\left(\frac{p_0}{p_5}\right)^{\frac{\gamma_g-1}{\gamma_g}}\right]} \tag{D1}$$

where

p_5 total pressure at turbine outlet, lb/sq ft absolute

The mass flow through the exhaust-nozzle area is expressed as

$$M_g=A_n\rho_5\left(\frac{p_0}{p_5}\right)^{\frac{1}{\gamma_g}}\sqrt{2Jc_{p,g}T_5\left[1-\left(\frac{p_0}{p_5}\right)^{\frac{\gamma_g-1}{\gamma_g}}\right]}$$

where

ρ_5 stagnation density at turbine outlet, slug/cu ft

Thus

$$\frac{M_g\sqrt{\theta_5}}{A_n\delta_5}=\frac{2116}{R_g\sqrt{519}}\left(\frac{p_0}{p_5}\right)^{\frac{1}{\gamma_g}}\sqrt{2Jc_{p,g}\left[1-\left(\frac{p_0}{p_5}\right)^{\frac{\gamma_g-1}{\gamma_g}}\right]} \tag{D2a}$$

Equation (D2a) is used until the critical pressure ratio is reached. The value of $\frac{M_g\sqrt{\theta_5}}{A_n\delta_5}$ remains constant thereafter as p_0/p_5 becomes less than the critical pressure ratio. The mass-flow-per-unit-area factor for critical flow is

$$\frac{M_g\sqrt{\theta_5}}{A_n\delta_5}=\frac{2116}{R_g\sqrt{519}}\sqrt{\frac{2\gamma_g}{\gamma_g+1}\left(\frac{2}{\gamma_g+1}\right)^{\frac{2}{\gamma_g-1}}} \tag{D2b}$$

From energy considerations

$$T_5=T_4-\frac{\eta_{t,s}V_t^2}{2Jc_{p,g}}$$

from which

$$\frac{\theta_5}{\theta_4}=1-\frac{\eta_{t,s}}{2Jc_{p,g}519}\left(\frac{V_t}{\sqrt{\theta_4}}\right)^2 \tag{D3}$$

The jet-velocity factor

$$\frac{V_i}{\sqrt{\theta_1}}=\frac{F}{M_a\sqrt{\theta_1}}+\frac{V_o}{\sqrt{\theta_1}}$$

which, when using equation (B14) and equation (15), becomes

$$\frac{V_i}{\sqrt{\theta_1}}=\frac{F}{M_a\sqrt{\theta_1}}+\sqrt{2Jc_{p,a}519\left(\frac{Y}{1+Y}\right)} \tag{D4}$$

The procedure for determining the design-point exhaust-nozzle area and the locus of the fixed-exhaust-nozzle-area curve is outlined in the next section and illustrated for the case of a turbojet engine with a centrifugal-flow compressor operating at a value of Y of 0.1.

DETERMINATION OF DESIGN EXHAUST-NOZZLE AREA

When an engine is equipped with a fixed-area exhaust nozzle, the size of the nozzle area used is generally that required for engine operation at the design point. This design exhaust-nozzle area is determined as follows:

1. Values corresponding to the desired design point for p_2/p_1, $U/\sqrt{\theta_1}$, T_4/T_1, $M_a\sqrt{\theta_1}/\delta_1$, K_c, and an approximate value of η_t are read from figure 13, and $F/M_a\sqrt{\theta_1}$ is read from figure 15 (b).

2. The approximate value of $\eta_{t,s}$ from figure 12 (b) that corresponds to the approximate value of η_t is used to compute an approximate value of u/V_t from equation (10).

3. For a given value of the ratio of combustion-chamber pressure drop to combustion-chamber-inlet pressure r, the approximate value of M_gV_t/δ_4 is computed from equation (C2).

4. The value of $V_t/\sqrt{\theta_4}$, corresponding to values of M_gV_t/δ_4 and u/V_t previously obtained, is read from figure 12 (a).

5. The value of $V_t/\sqrt{\theta_4}$ is used in equation (D3) to calculate θ_5/θ_4.

6. Using the values of $F/M_a\sqrt{\theta_1}$ and Y in equation (D4) gives $V_i/\sqrt{\theta_1}$.

7. From the identity

$$\frac{V_i}{\sqrt{\theta_5}}=\frac{V_i}{\sqrt{\theta_1}}\sqrt{\frac{\theta_4}{\theta_5}}\sqrt{\frac{T_1}{T_4}}$$

$V_i/\sqrt{\theta_5}$ is calculated. Using this value in equation (D1) determines p_0/p_5.

8. Using the value of p_0/p_5 in equation (D2a) gives $\frac{M_g\sqrt{\theta_5}}{A_n\delta_5}$. If the value of p_0/p_5 is less than the critical pressure ratio, then the same value of $\frac{M_g\sqrt{\theta_5}}{A_n\delta_5}$ as occurs at the critical pressure ratio is used. This critical value of $\frac{M_g\sqrt{\theta_5}}{A_n\delta_5}$ is obtained from equation (D2b).

9. With a ram pressure loss assumed, the value of p_1/p_0 is determined from the value of Y and equation (B16).

10. The value of A_n is then calculated from the identity

$$A_n=\frac{\left(\frac{M_a\sqrt{\theta_1}}{\delta_1}\right)\sqrt{\frac{T_4}{T_1}\frac{\theta_5}{\theta_4}}}{\left(\frac{M_g\sqrt{\theta_5}}{A_n\delta_5}\right)\left(\frac{p_5}{p_0}\right)\left(\frac{p_0}{p_1}\right)}$$

DETERMINATION OF FIXED-EXHAUST-NOZZLE-AREA CURVE

Once the design area has been found, the operational points of the engine with the fixed-exhaust-nozzle area A_n have to be determined at other rotational speeds. At any given $U/\sqrt{\theta_1}$, the exhaust-nozzle areas required for several operating points are determined by the method just outlined. The operating point corresponding to the design A_n at a given $U/\sqrt{\theta_1}$ is then determined by interpolation. This process is repeated for a sufficient range of values of $U/\sqrt{\theta_1}$ and the line of fixed A_n is located. The difference between M_a and M_g was neglected in this procedure.

In order to obtain the operating line of fixed A_n for another flight speed, the procedure is repeated using the new value for Y.

In order to illustrate the method, the exhaust-nozzle area for the engine with a centrifugal-flow compressor is evaluated for a design value of Y of 0.1 as follows:

1. From figure 13, design-point conditions are: p_2/p_1, 4.12; T_4/T_1, 4.0; $M_a\sqrt{\theta_1}/\delta_1$, 1.96 (slug/sec); K_c, 0.91; $U/\sqrt{\theta_1}$, 1600 (ft/sec); η_t, 0.85; and from figure 15 (b) the corresponding $F/M_a\sqrt{\theta_1}$ is 1272 (lb/(slug/sec)).

2. Corresponding to η_t of 0.85, a value of $\eta_{t,s}$ of 0.80 is obtained from figure 12 (b). A value of u/V_t of 0.52 is evaluated from equation (10).

3. For a value of r of 0.05, the value of M_gV_t/δ_4 evaluated from equation (C2) is 1209 ((slug)(ft)/sec^2).

4. From figure 12 (a), corresponding to this value of M_gV_t/δ_4, the values of $V_t/\sqrt{\theta_4}$ of 1209 (ft/sec) and $p_4/p_{5,s}$ of 2.50 are obtained. The $p_4/p_{5,s}$ value indicates that the flow through the turbine is sonic.

5. A value of $c_{p,g}$ of 8.6 (Btu/(slug)(°F)) is assumed; then from equation (D3), the value of θ_5/θ_4 of 0.831 is obtained.

6. Values of $F/M_a\sqrt{\theta_1}$ and Y used in equation (D4) result in a value of $V_j/\sqrt{\theta_1}$ of 2025 (ft/sec).

7. A value of $V_j/C_v\sqrt{\theta_5}$ of 1142 (ft/sec) is determined from the values of $V_j/\sqrt{\theta_1}$, θ_5/θ_4, and T_4/T_1, and a value of C_v chosen as 0.97. Corresponding to this value of $V_j/C_v\sqrt{\theta_5}$, the p_5/p_0 determined from equation (D1) is 2.25, which is greater than critical pressure ratio indicating that the flow through the exhaust nozzle is sonic.

8. From equation (D2b) and values of γ of 1.35 and R_g of 1720 (ft-lb/(slug)(°F)), the critical $M_g\sqrt{\theta_5}/A_n\delta_5$ of 1.516 ((slug/sec)/sq ft) is determined.

9. The ideal ram pressure ratio $p_{1,i}/p_0$, obtained using the value of Y in equation (B16), is 1.396. With an inlet-duct pressure loss $\Delta p_d/p_0$ of 0.04 assumed, then p_1/p_0 is 1.356.

10. From the identity

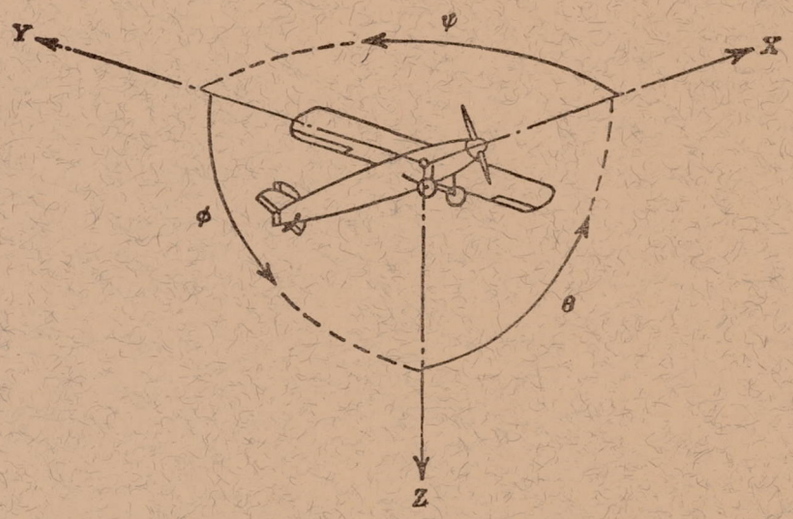
$$A_n=\frac{\left(\frac{M_a\sqrt{\theta_1}}{\delta_1}\right)\sqrt{\frac{T_4}{T_1}\frac{\theta_5}{\theta_4}}}{\left(\frac{M_g\sqrt{\theta_5}}{A_n\delta_5}\right)\left(\frac{p_5}{p_0}\right)\left(\frac{p_0}{p_1}\right)}$$

a value of A_n of 1.42 square feet is obtained.

REFERENCES

1. Keirn, D. J., and Shoults, D. R.: Jet Propulsion and Its Application to High-Speed Aircraft. Jour. Aero. Sci., vol. 13, no. 8, Aug. 1946, pp. 411–424.
2. Bolz, Ray E.: Graphical Solution for the Performance of Continuous-Flow Jet Engines. SAE Quarterly Trans., vol. 1, no. 2, April 1947, pp. 235–251.
3. Rubert, Kennedy F.: An Analysis of Jet-Propulsion Systems Making Direct Use of the Working Substance of a Thermodynamic Cycle. NACA ACR No. L5A30a, 1945.
4. Palmer, Carl B.: Performance of Compressor-Turbine Jet-Propulsion Systems. NACA ACR No. L5E17, 1945.
5. Hawthorne, William R.: Factors Affecting the Design of Jet Turbines. SAE Jour. (Trans.), vol. 54, no. 7, July 1946, pp. 347–357; discussion, p. 357.
6. Keenan, Joseph H., and Kaye, Joseph: Thermodynamic Properties of Air. John Wiley & Sons, Inc., 1945.
7. Turner, L. Richard, and Lord, Albert M.: Thermodynamic Charts for the Computation of Combustion and Mixture Temperatures at Constant Pressure. NACA TN No. 1086, 1946.
8. Pinkel, Benjamin, and Turner, L. Richard: Thermodynamic Data for the Computation of the Performance of Exhaust-Gas Turbines. NACA ARR No. 4B25, 1944.

U. S GOVERNMENT PRINTING OFFICE: 1949



Positive directions of axes and angles (forces and moments) are shown by arrows

Axis		Force (parallel to axis) symbol	Moment about axis			Angle		Velocities	
Designation	Symbol		Designation	Symbol	Positive direction	Designation	Symbol	Linear (component along axis)	Angular
Longitudinal	X	X	Rolling	L	$Y \longrightarrow Z$	Roll	ϕ	u	p
Lateral	Y	Y	Pitching	M	$Z \longrightarrow X$	Pitch	θ	v	q
Normal	Z	Z	Yawing	N	$X \longrightarrow Y$	Yaw	ψ	w	r

Absolute coefficients of moment

$C_l = \frac{L}{qbS}$ (rolling) $\quad C_m = \frac{M}{qcS}$ (pitching) $\quad C_n = \frac{N}{qbS}$ (yawing)

Angle of set of control surface (relative to neutral position), δ. (Indicate surface by proper subscript.)

4. PROPELLER SYMBOLS

D Diameter

p Geometric pitch

p/D Pitch ratio

V' Inflow velocity

V_s Slipstream velocity

T Thrust, absolute coefficient $C_T = \frac{T}{\rho n^2 D^4}$

Q Torque, absolute coefficient $C_Q = \frac{Q}{\rho n^2 D^5}$

P Power, absolute coefficient $C_P = \frac{P}{\rho n^3 D^5}$

C_s Speed-power coefficient $= \sqrt[5]{\frac{\rho V^5}{P n^2}}$

η Efficiency

n Revolutions per second, rps

Φ Effective helix angle $= \tan^{-1}\left(\frac{V}{2\pi r n}\right)$

5. NUMERICAL RELATIONS

1 hp=76.04 kg-m/s=550 ft-lb/sec

1 metric horsepower=0.9863 hp

1 mph=0.4470 mps

1 mps=2.2369 mph

1 lb=0.4536 kg

1 kg=2.2046 lb

1 mi=1,609.35 m=5,280 ft

1 m=3.2808 ft